LHAASO宇宙线分成分能谱测量

进展和未来展望

张寿山

代表 LHAASO 合作组

中国科学院高能物理研究所

粒子天体物理全国重点实验室

高能宇宙线物理及下一代空间探测装置研讨会，Jul 30 – Aug 3, 2025

The Site

Bird’s eye view of LHAASO， 2021-08

- Location： 29o21’ 27.6” N , 100o08’19.6” E
- Altitude: 4410 m
- 2021-07 completed built and in operation

LHAASO, *Nature Astronomy* *5:849 (2021)*

(Aug. 2018, at 4410 m a.s.l.)

LHAASO: Multi-Messenger Collaboration Network

The LHAASO collaboration has signed MOUs with 8 international detector collaboration.

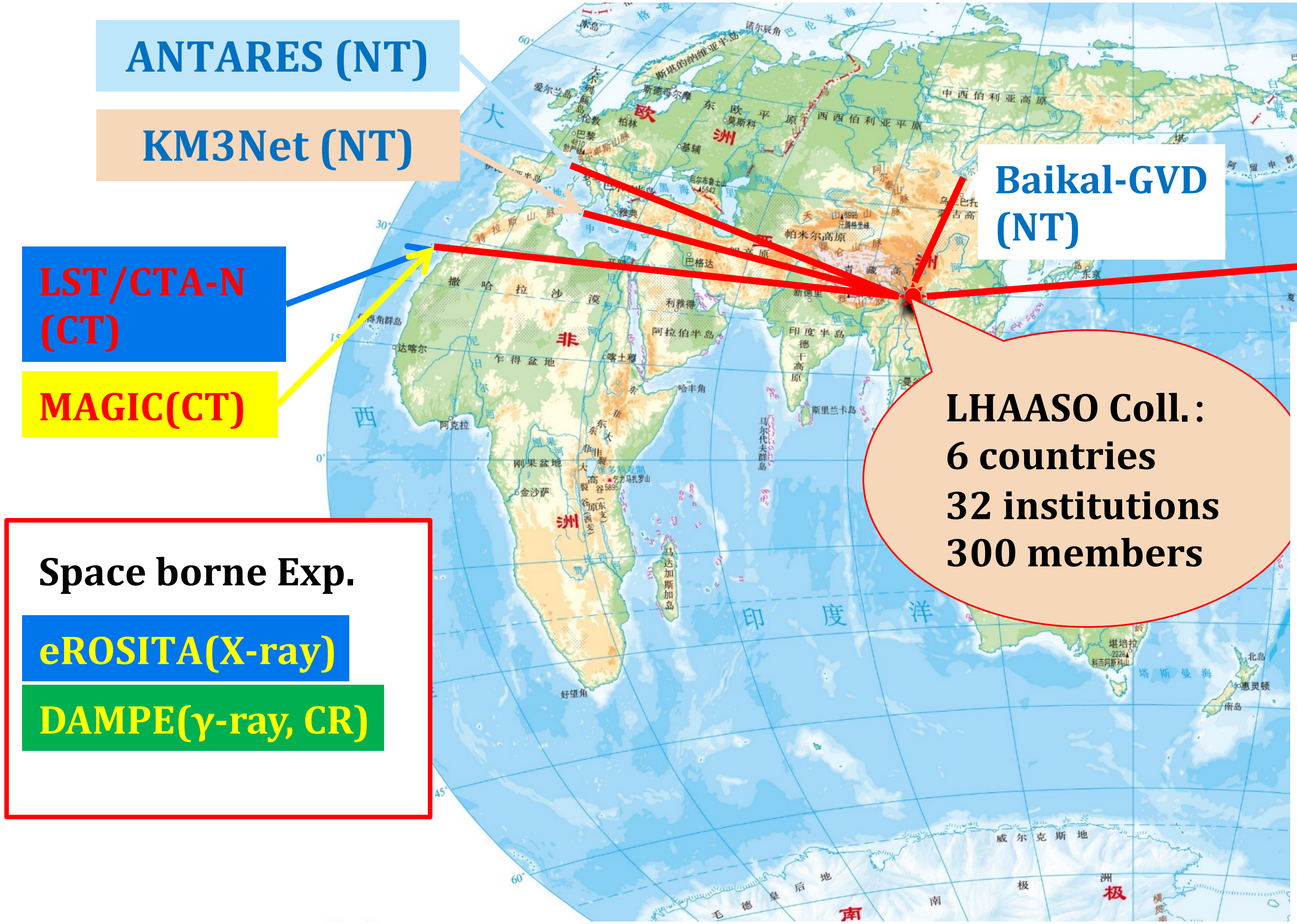

Zhen Cao,[1,2,3] F. Aharonian,[4,5] Q. An,[6,7] Axikegu,[8] L.X. Bai,[9] Y.X. Bai,[1,3] Y.W. Bao,[10] D. Bastieri,[11] X.J. Bi*,[1,2,3] Y.J. Bi,[1,3] H. Cai,[12] J.T. Cai,[11] Zhe Cao,[6,7] J. Chang,[13] J.F. Chang,[1,3,6] B.M. Chen,[14] E.S. Chen*,[1,2,3] J. Chen,[9] Liang Chen,[1,2,3] Liang Chen,[15] Long Chen,[8] M.J. Chen,[1,3] M.L. Chen,[1,3,6] Q.H. Chen,[8] S.H. Chen,[1,2,3] S.Z. Chen,[1,3] T.L. Chen,[16] X.L. Chen,[1,2,3] Y. Chen,[10] N. Cheng,[1,3] Y.D. Cheng,[1,3] S.W. Cui,[14] X.H. Cui,[17] Y.D. Cui,[18] B. D'Ettorre Piazzoli,[19] B.Z. Dai,[20] H.L. Dai,[1,3,6] Z.G. Dai,[7] Danzengluobu,[16] D. della Volpe,[21] X.J. Dong,[1,3] K.K. Duan,[13] J.H. Fan,[11] Y.Z. Fan,[13] Z.X. Fan,[1,3] J. Fang,[20] K. Fang,[1,3] C.F. Feng,[22] L. Feng,[13] S.H. Feng,[1,3] Y.L. Feng,[13] B. Gao,[1,3] C.D. Gao,[22] L.Q. Gao*,[1,2,3] Q. Gao,[16] W. Gao,[22] M.M. Ge,[20] L.S. Geng,[1,3] G.H. Gong,[23] Q.B. Gou,[1,3] M.H. Gu,[1,3,6] F.L. Guo,[15] J.G. Guo,[1,2,3] X.L. Guo,[8] Y.Q. Guo,[1,3] Y.Y. Guo,[1,2,3,13] Y.A. Han,[24] H.H. He,[1,2,3] H.N. He,[13] J.C. He,[1,2,3] S.L. He,[11] X.B. He,[18] Y. He,[8] M. Heller,[21] Y.K. Hor,[18] C. Hou,[1,3] X. Hou,[25] H.B. Hu,[1,2,3] S. Hu,[9] S.C. Hu,[1,2,3] X.J. Hu,[23] D.H. Huang,[8] Q.L. Huang,[1,3] W.H. Huang,[22] X.T. Huang,[22] X.Y. Huang,[13] Z.C. Huang,[8] F. Ji,[1,3] X.L. Ji,[1,3,6] H.Y. Jia,[8] K. Jiang,[6,7] Z.J. Jiang,[20] C. Jin,[1,2,3] T. Ke,[1,3] D. Kuleshov,[26] K. Levochkin,[26] B.B. Li,[14] Cheng Li,[6,7] Cong Li,[1,3] F. Li,[1,3,6] H.B. Li,[1,3] H.C. Li,[1,3] H.Y. Li,[7,13] Jian Li,[7] Jie Li,[1,3,6] K. Li,[1,3] W.L. Li,[22] X.R. Li,[1,3] Xin Li,[6,7] Xin Li,[8] Y. Li,[9] Y.Z. Li,[1,2,3] Zhe Li,[1,3] Zhuo Li,[27] E.W. Liang,[28] Y.F. Liang,[28] S.J. Lin,[18] B. Liu,[7] C. Liu,[1,3] D. Liu,[22] H. Liu,[8] H.D. Liu,[24] J. Liu,[1,3] J.L. Liu,[29] J.S. Liu,[18] J.Y. Liu,[1,3] M.Y. Liu,[16] R.Y. Liu,[10] S.M. Liu,[8] W. Liu,[1,3] Y. Liu,[11] Y.N. Liu,[23] Z.X. Liu,[9] W.J. Long,[8] R. Lu,[20] H.K. Lv,[1,3] B.Q. Ma,[27] L.L. Ma,[1,3] X.H. Ma,[1,3] J.R. Mao,[25] A. Masood,[8] Z. Min,[1,3] W. Mitthumsiri,[30] T. Montaruli,[21] Y.C. Nan,[22] B.Y. Pang,[8] P. Pattarakijwanich,[30] Z.Y. Pei,[11] M.Y. Qi,[1,3] Y.Q. Qi,[14] B.Q. Qiao,[1,3] J.J. Qin,[7] D. Ruffolo,[30] V. Rulev,[26] A. Sáiz,[30] L. Shao,[14] O. Shchegolev,[26,31] X.D. Sheng,[1,3] J.R. Shi,[1,3] H.C. Song,[27] Yu.V. Stenkin,[26,31] V. Stepanov,[26] Y. Su,[13] Q.N. Sun,[8] X.N. Sun,[28] Z.B. Sun,[32] P.H.T. Tam,[18] Z.B. Tang,[6,7] W.W. Tian,[2,17] B.D. Wang,[1,3] C. Wang,[32] H. Wang,[8] H.G. Wang,[11] J.C. Wang,[25] J.S. Wang,[29] L.P. Wang,[22] L.Y. Wang,[1,3] R.N. Wang,[8] W. Wang,[18] W. Wang,[12] X.G. Wang,[28] X.J. Wang,[1,3] X.Y. Wang,[10] Y. Wang,[8] Y.D. Wang,[1,3] Y.J. Wang,[1,3] Y.P. Wang,[1,2,3] Z.H. Wang,[9] Z.X. Wang,[20] Zhen Wang,[29] Zheng Wang,[1,3,6] D.M. Wei,[13] J.J. Wei,[13] Y.J. Wei,[1,2,3] T. Wen,[20] C.Y. Wu,[1,3] H.R. Wu,[1,3] S. Wu,[1,3] W.X. Wu,[8] X.F. Wu,[13] S.Q. Xi,[1,3] J. Xia,[7,13] J.J. Xia,[8] G.M. Xiang,[2,15] D.X. Xiao,[16] G. Xiao,[1,3] H.B. Xiao,[11] G.G. Xin,[12] Y.L. Xin,[8] Y. Xing,[15] D.L. Xu,[29] R.X. Xu,[27] L. Xue,[22] D.H. Yan,[25] J.Z. Yan,[13] C.W. Yang,[9] F.F. Yang,[1,3,6] J.Y. Yang,[18] L.L. Yang,[18] M.J. Yang,[1,3] R.Z. Yang,[7] S.B. Yang,[20] Y.H. Yao,[9] Z.G. Yao,[1,3] Y.M. Ye,[23] L.Q. Yin,[1,3] N. Yin,[22] X.H. You,[1,3] Z.Y. You,[1,2,3] Y.H. Yu,[22] Q. Yuan*,[13] H.D. Zeng,[13] T.X. Zeng,[1,3,6] W. Zeng,[20] Z.K. Zeng,[1,2,3] M. Zha,[1,3] X.X. Zhai,[1,3] B.B. Zhang,[10] H.M. Zhang,[10] H.Y. Zhang,[22] J.L. Zhang,[17] J.W. Zhang,[9] L.X. Zhang,[11] Li Zhang,[20] Lu Zhang,[14] P.F. Zhang,[20] P.P. Zhang,[14] R. Zhang,[7,13] S.R. Zhang,[14] S.S. Zhang,[1,3] X. Zhang,[10] X.P. Zhang,[1,3] Y.F. Zhang,[8] Y.L. Zhang,[1,3] Yi Zhang*,[1,13] Yong Zhang,[1,3] B. Zhao,[8] J. Zhao,[1,3] L. Zhao,[6,7] L.Z. Zhao,[14] S.P. Zhao*,[13,22] F. Zheng,[32] Y. Zheng,[8] B. Zhou,[1,3] H. Zhou,[29] J.N. Zhou,[15] P. Zhou,[10] R. Zhou,[9] X.X. Zhou,[8] C.G. Zhu,[22] F.R. Zhu,[8] H. Zhu,[17] K.J. Zhu,[1,2,3,6] and X. Zuo[1,3]

High Energy Cosmic Rays

Large High Altitude Air Shower Observatory (LHAASO)

CATCHING RAYS

China's new observatory will intercept ultra-high-energy γ-ray particles and cosmic rays.

LHAASO Physics Topics

- Gamma Ray Astronomy
- Charged CRs measurement
- New Physics Frontier

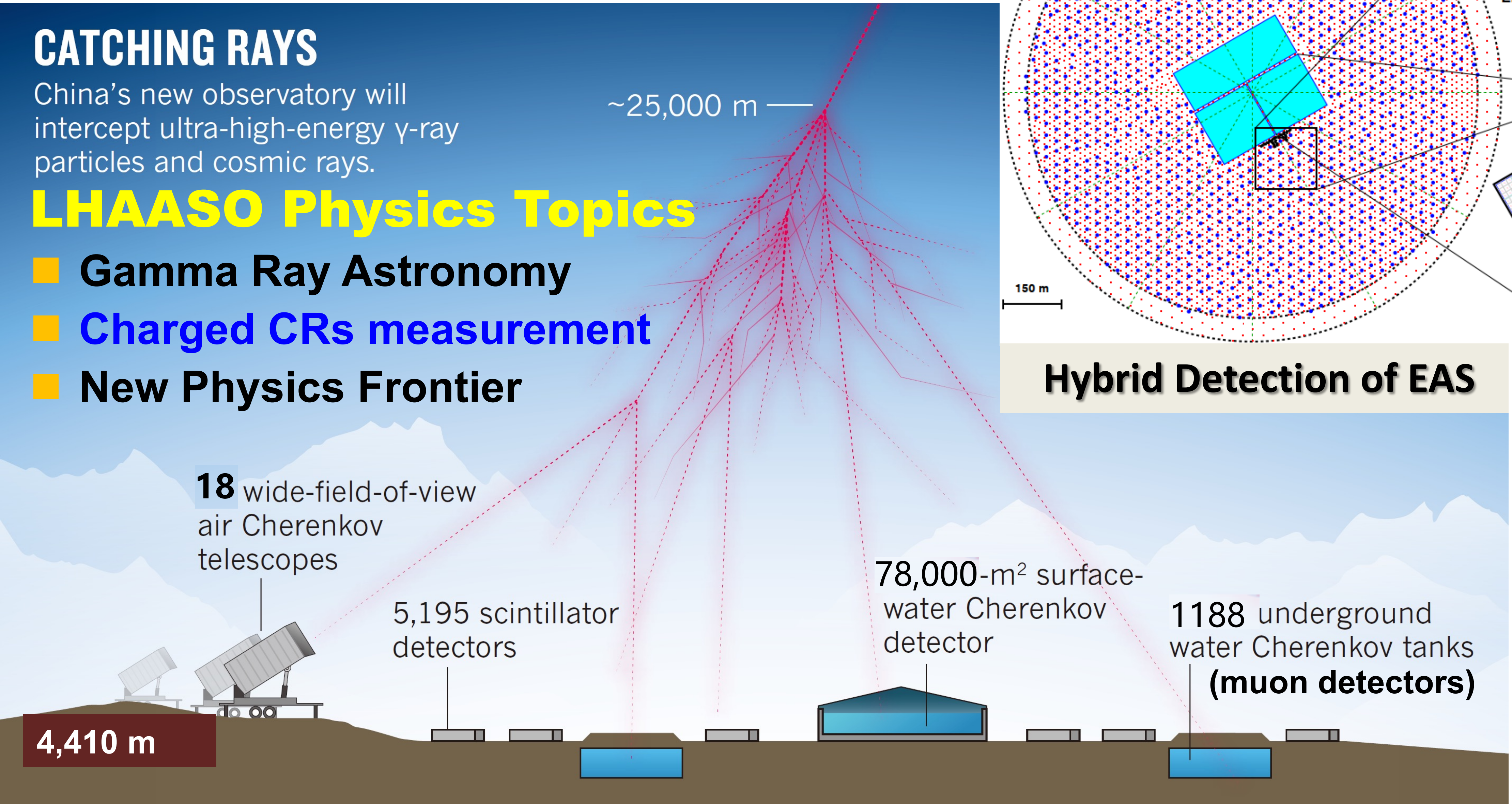

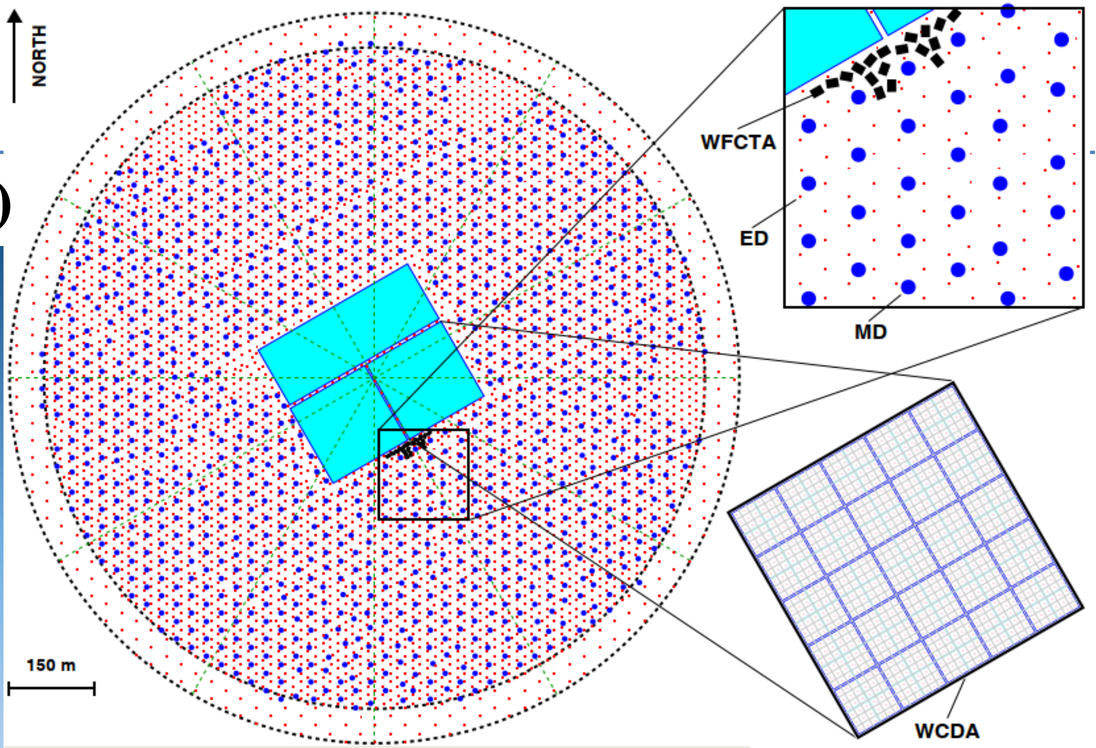

Hybrid Detection of EAS

Outline

- Introduction
- Proton energy spectrum measurement results in the knee region
- All particle energy spectrum and mass
- Progress in the helium and iron energy spectrum
- Summary & Outlook

Cosmic rays

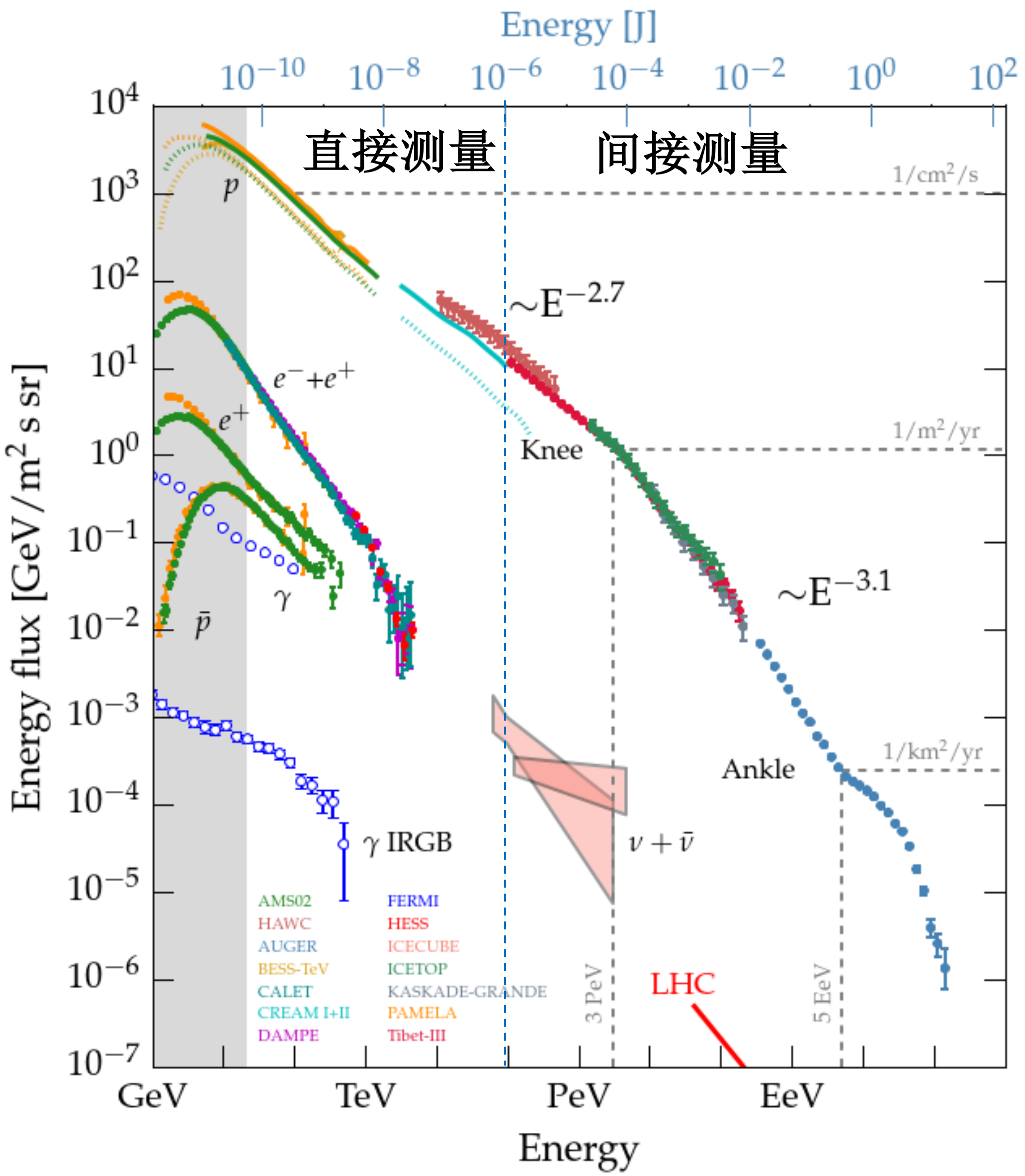

C.Evoli 10.5281/zenodo.1468853

- Proton, helium nuclei and heavier nuclei , all the way to uranium
- Discovered in 1912, many things (e.g. source, acceleration mechanism) about cosmic rays remain a mystery more than a century later
- Individual energy spectra play am important role to solve the mystery
  - Proton knee, helium knee, iron knee …
  - The knee indicates the energy limit for cosmic ray acceleration by astrophysical sources.

- **KASCADE experiment**
  - **Altitude： 110m**
  - **Unfolding： μ and electron matrix**
  - **The results strongly depend on the hadronic interaction models**
- **Individual components of CRs energy spectrum measurement are very important, but not easy.**

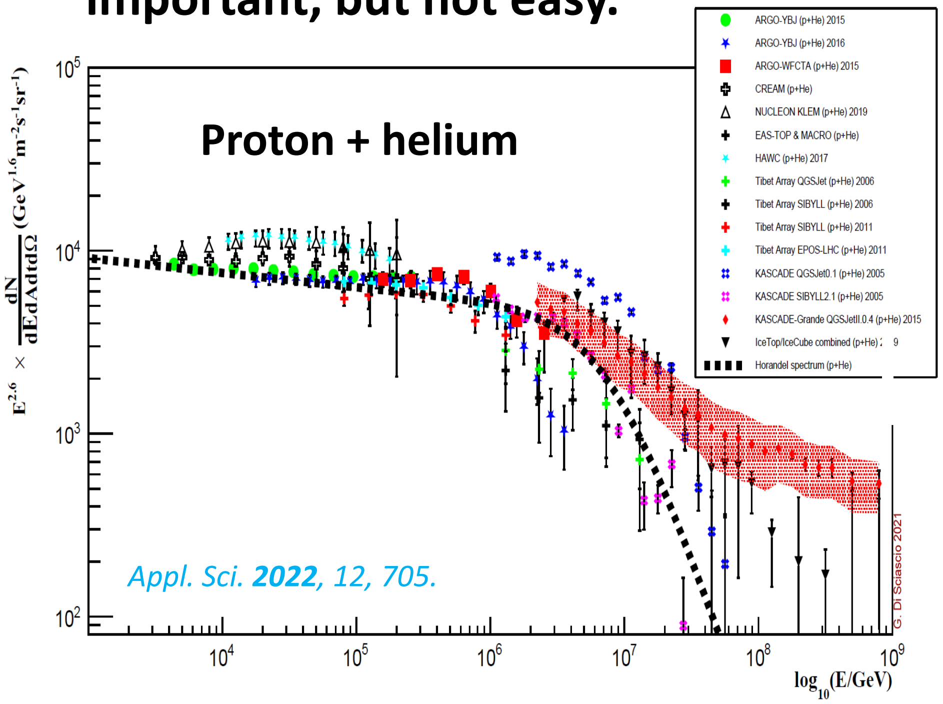

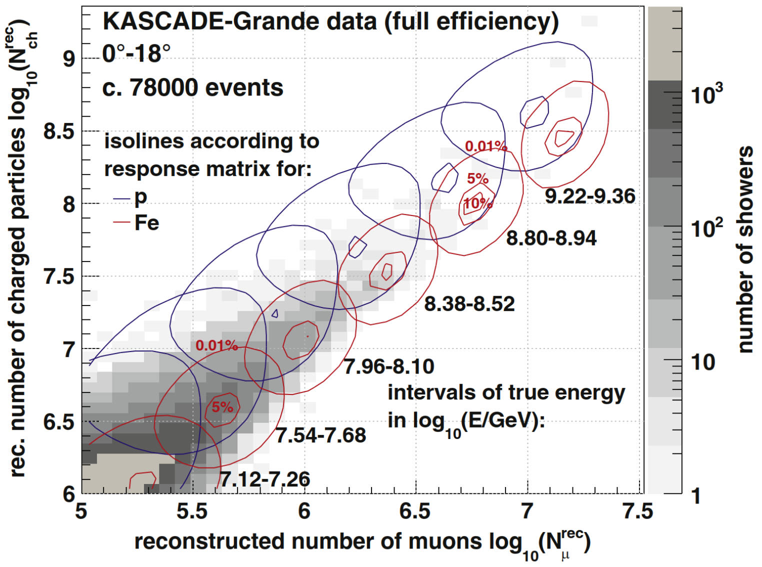

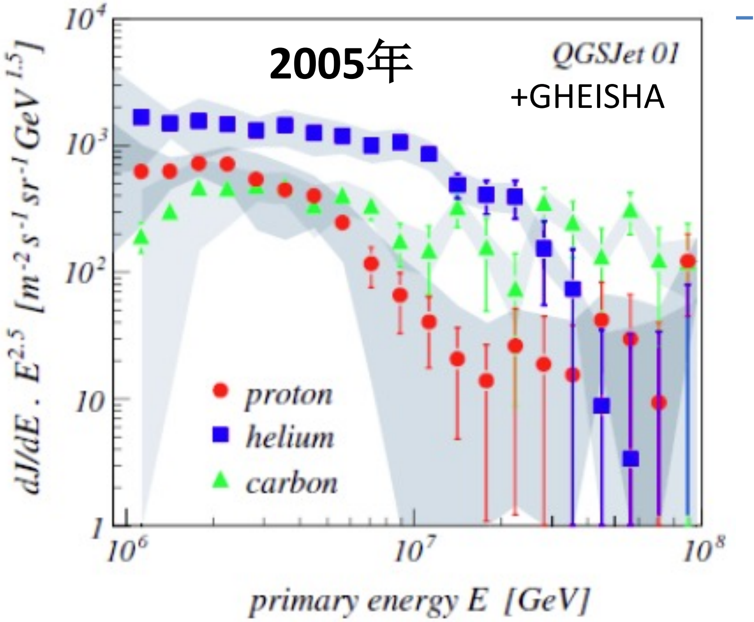

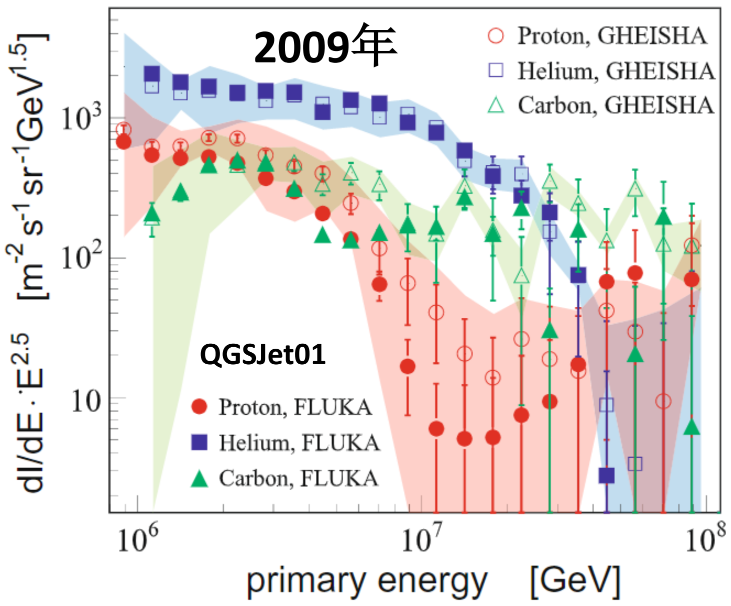

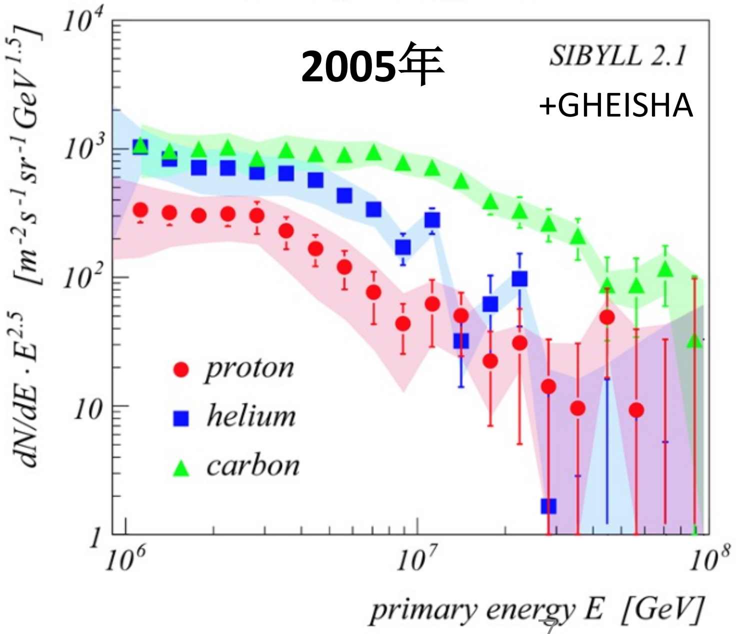

Hybrid Detection of EAS

高海拔宇宙线观测站（LHAASO）

- 地点：四川甘孜州稻城海子山
- 海拔: 4410 m

  “膝区”宇宙线测量的理想位置，测量精度高
- **2021年7月全阵列运行，2023年5月通过国家验收**

地面粒子探测器阵列(KM2A)

最灵敏的超高能伽马望远镜

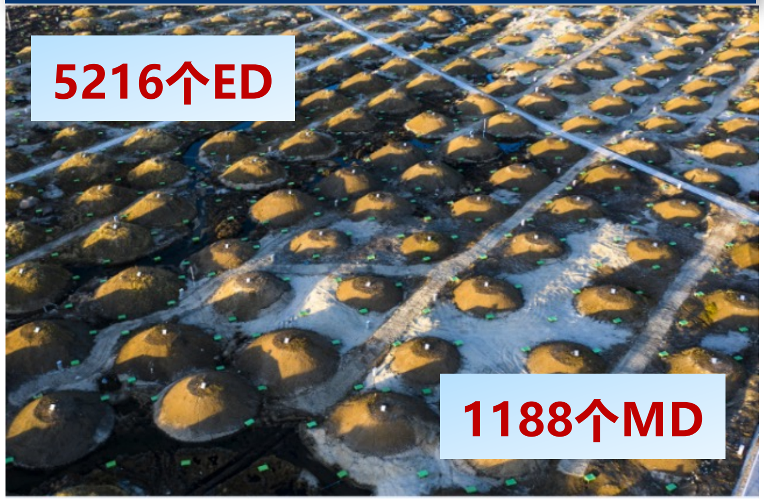

水切伦科夫探测器阵列(WCDA)

最灵敏的甚高能伽马巡天望远镜

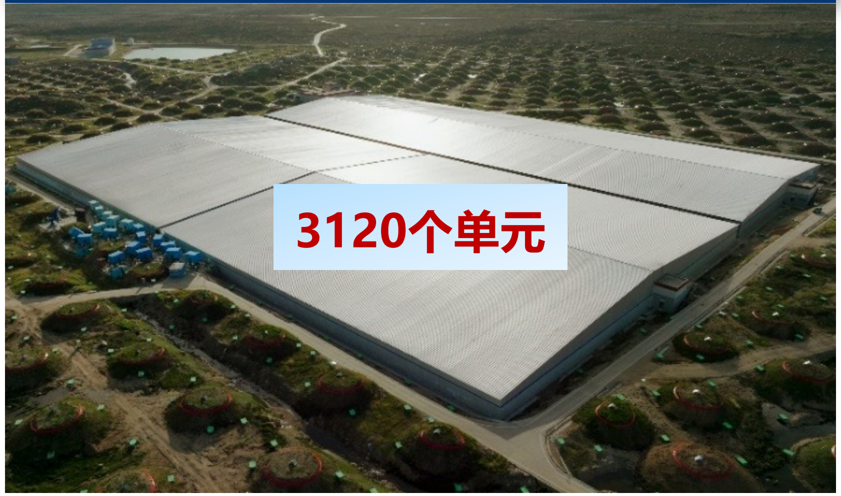

广角切伦科夫望远镜阵列(WFCTA)

能量覆盖最宽的高能宇宙线立体装置

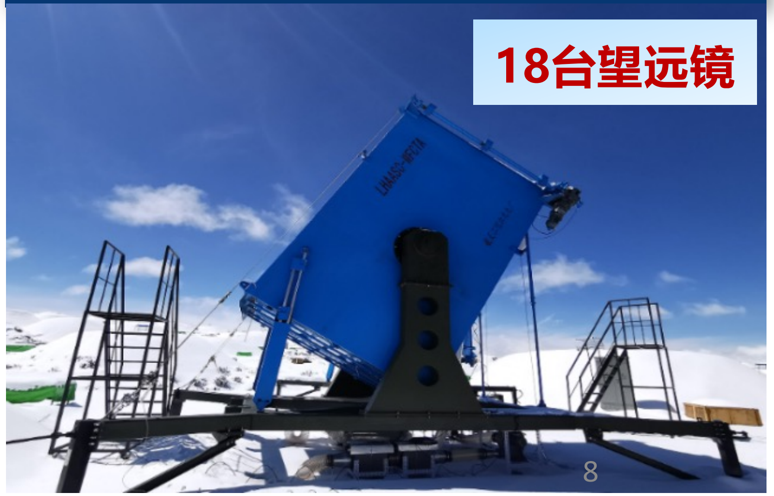

Hybrid Detection of EAS

宇宙线

质子，氦核，铁核等核子

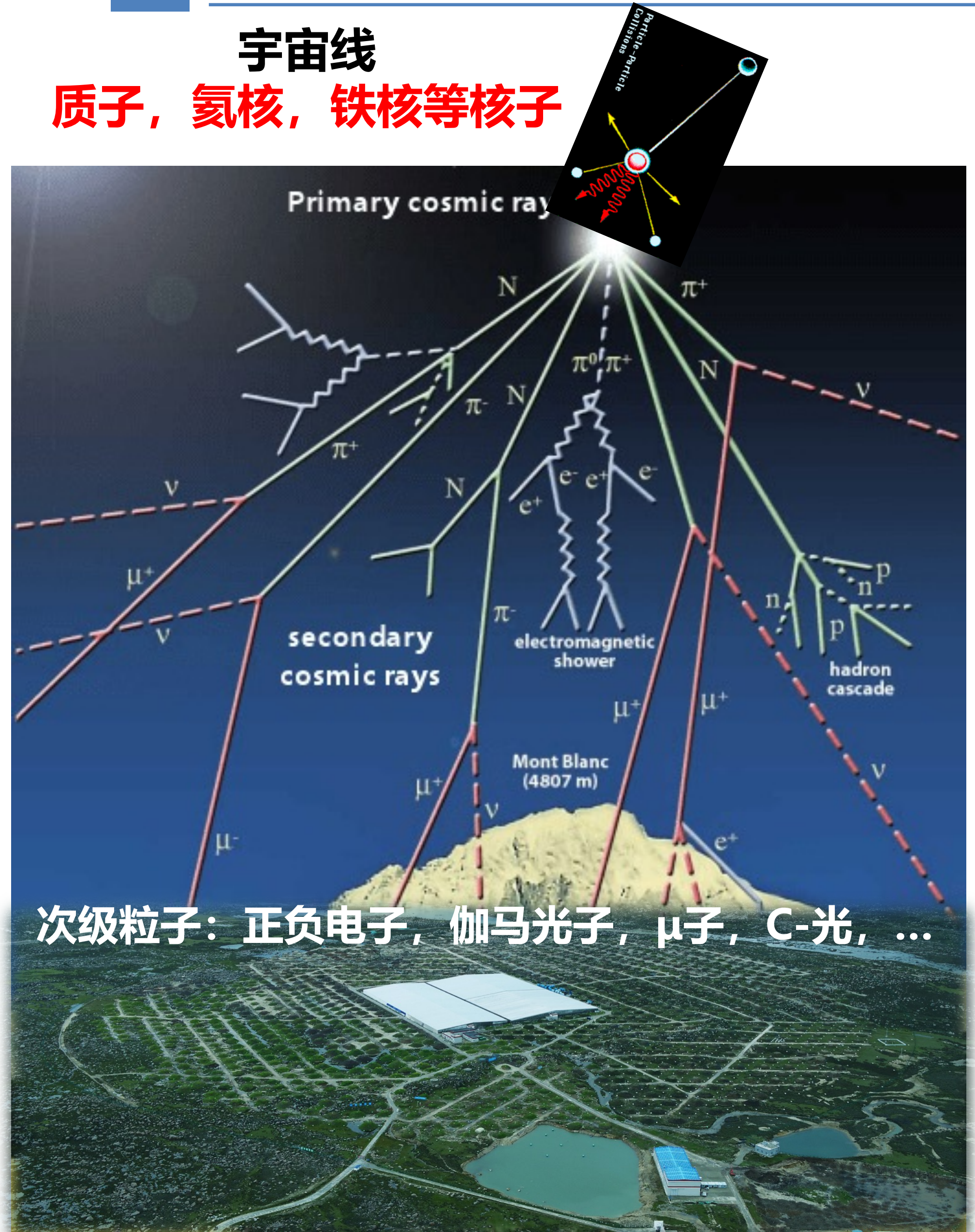

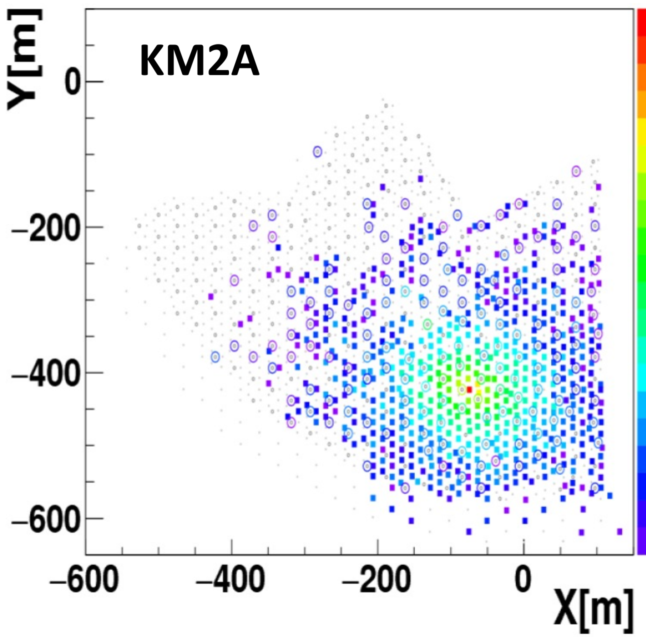

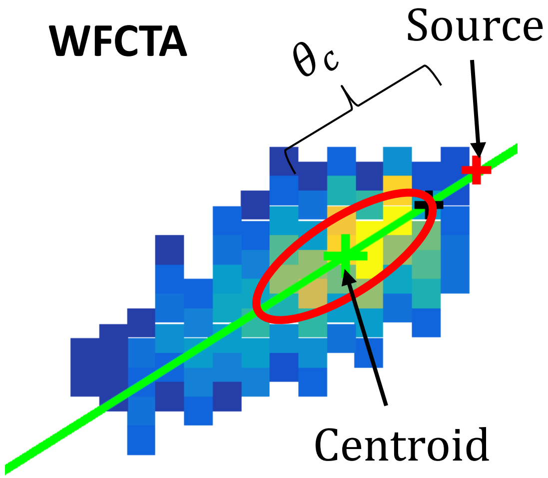

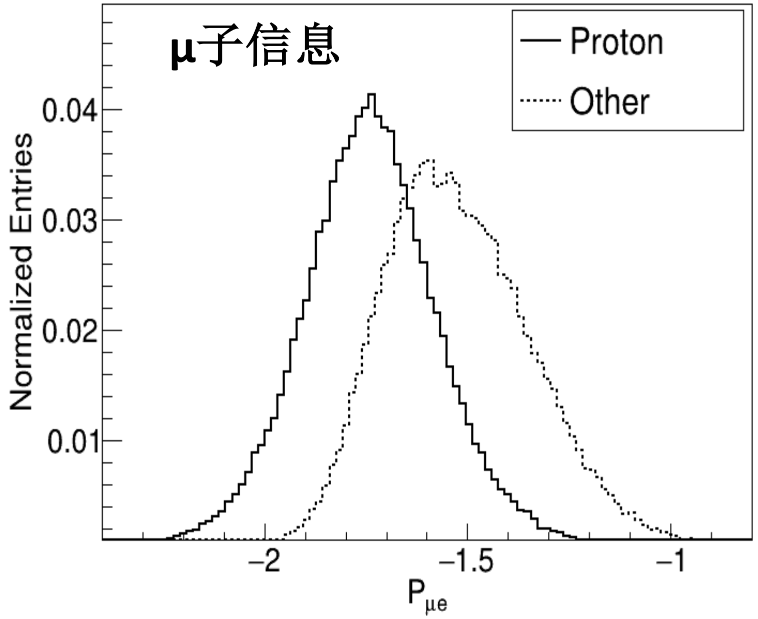

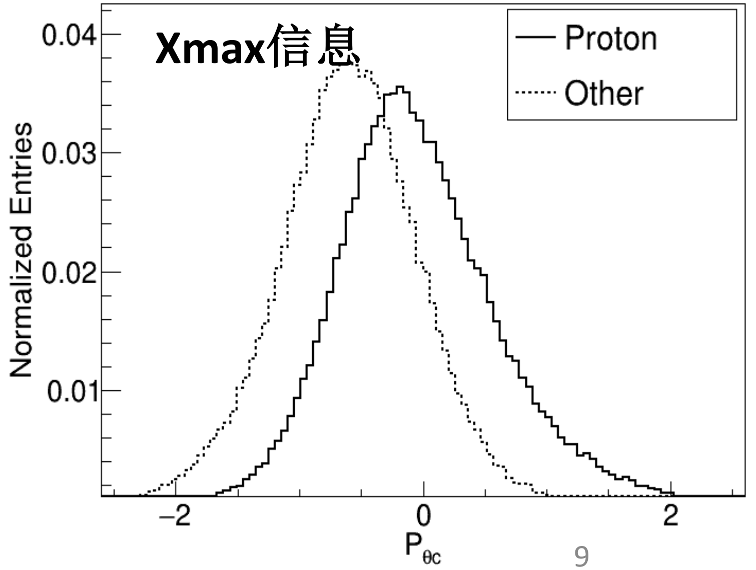

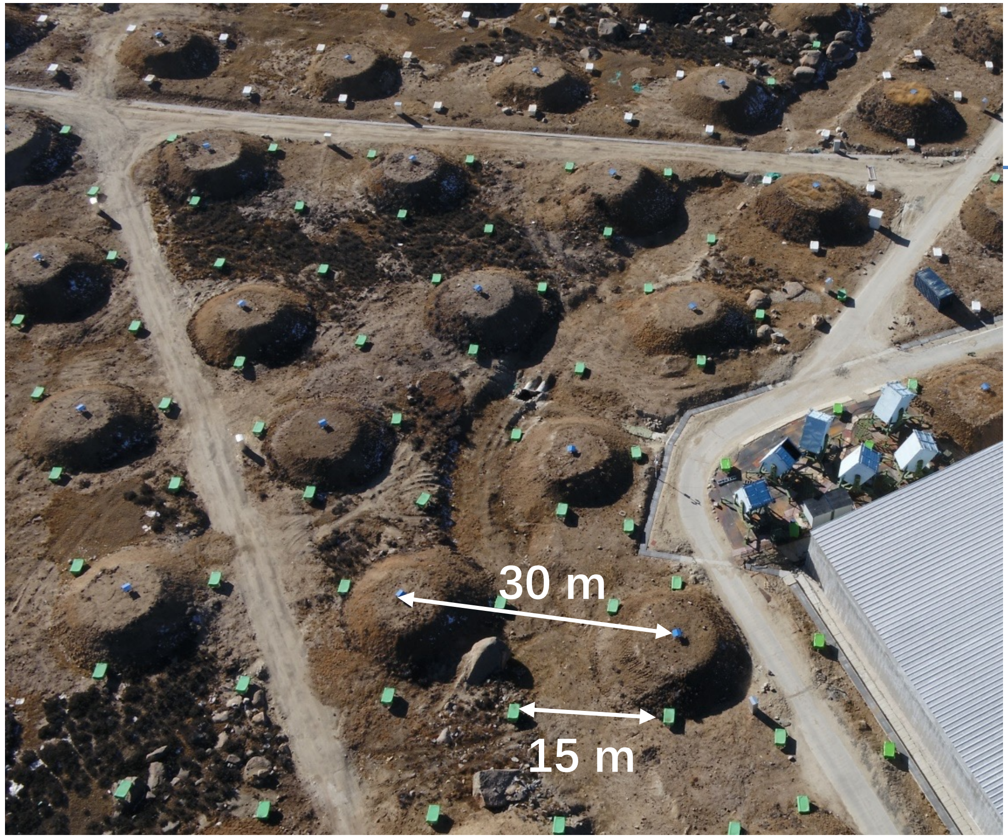

KM2A: 1.36 $(km)^2$

- 5195 EDs
  - 1 m^2 each
  - 15 m spacing
- 1188 MDs
  - 36 m^2 each
  - 30 m spacing

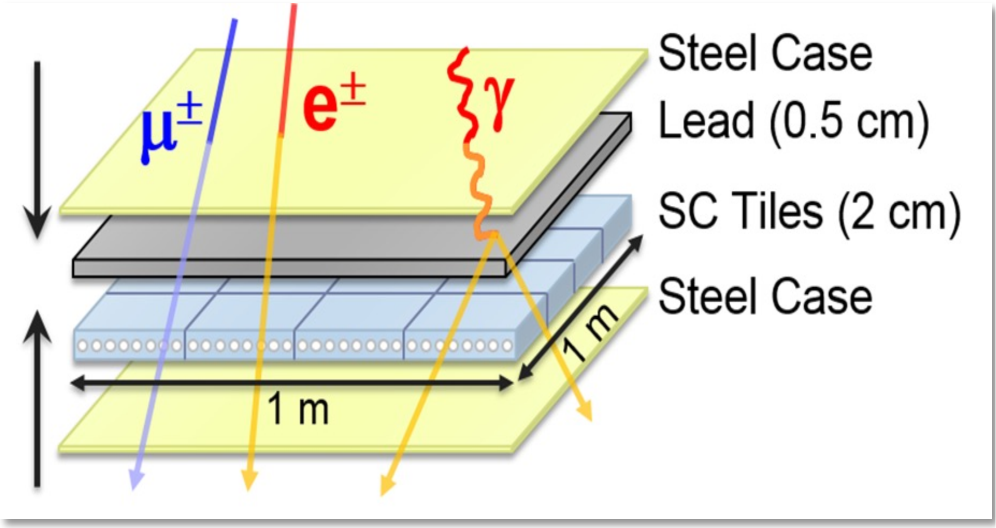

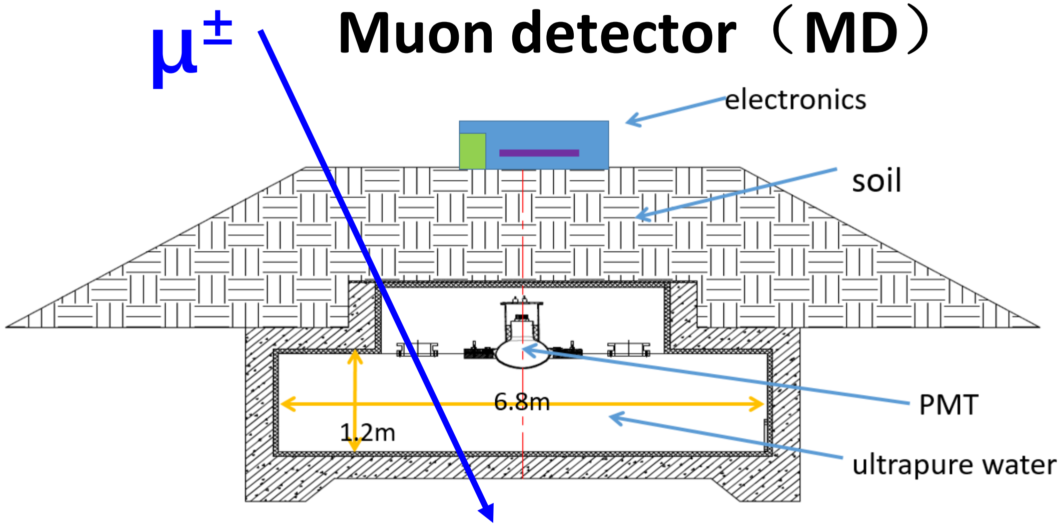

Inner View of one ED

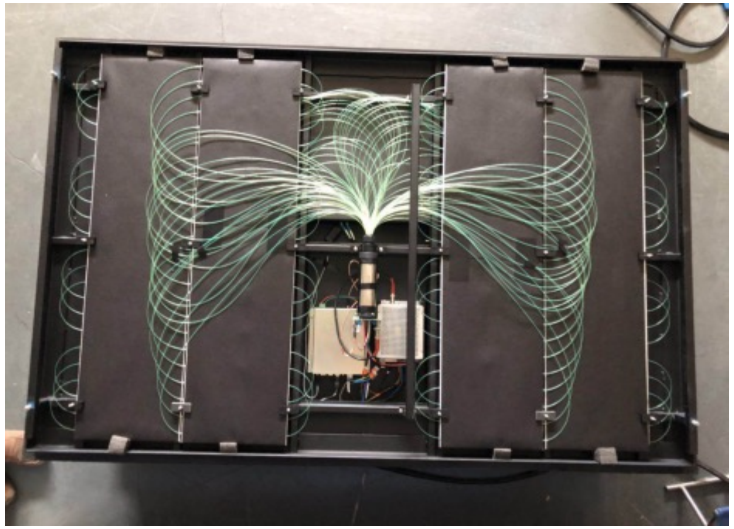

Wide Field of View Cherenkov Telescope (WFCTA)

- **Telescope parameters:**
  - ~5 m^2 spherical mirror
  - Camera: 32×32 SiPMs array
  - FOV: 16° × 16°
  - Pixel size: 0.5°
- **18 tels are pointed at a zenith angle of 45° cover azimuth angle from 0° to 360°**

Mirror

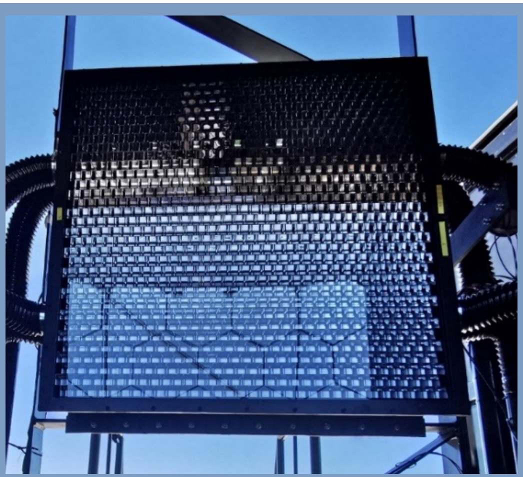

SiPM camera

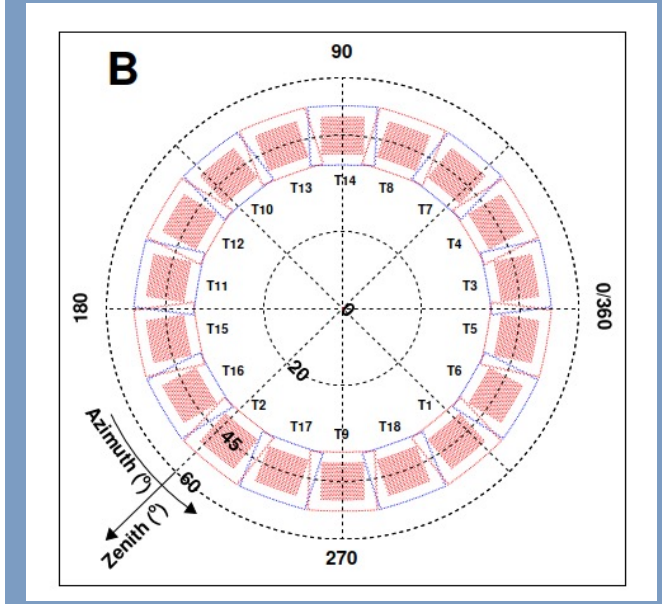

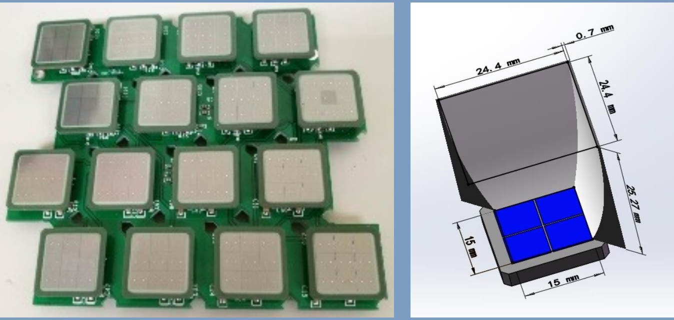

SiPM and Winstone cone

Water Cherenkov Detector Array (WCDA)

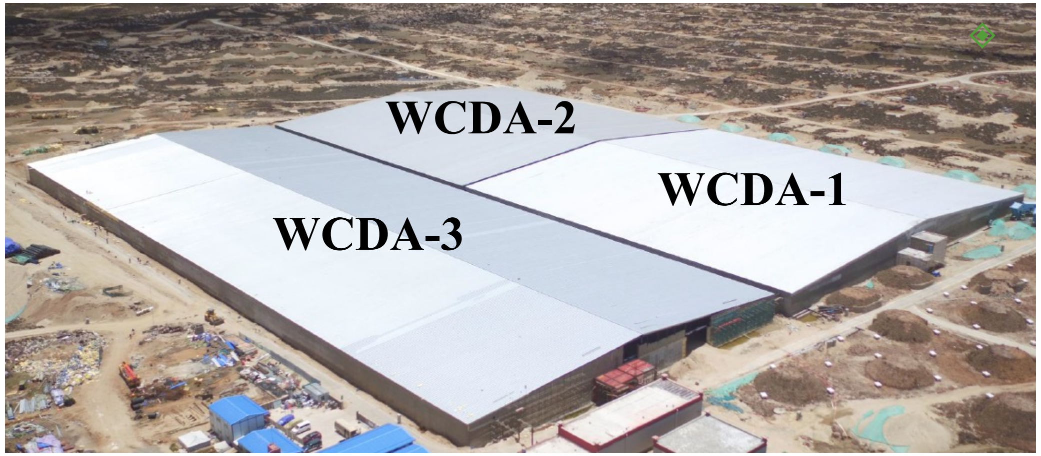

Energy rang

- WCDA-1
  - 300 GeV – 10 PeV
- WCDA-2 and WCDA-3
  - 100 GeV - 10 TeV

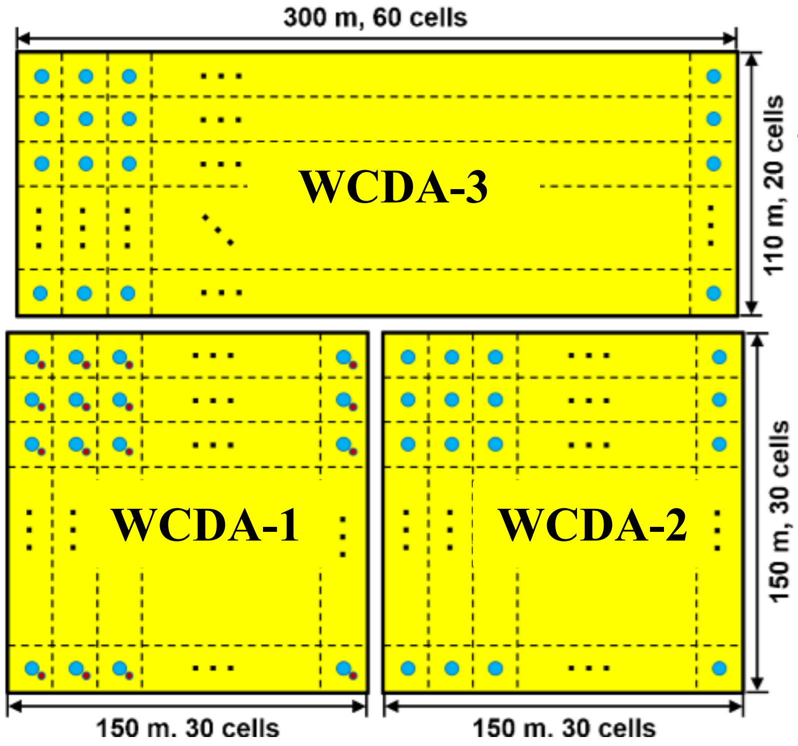

- Total area: $78,000m^2$
- Total units: 3,120
- Unit size: $5m \times 5m \times 4.4m$
- Two type of PMTs in each unit:
  - 8 inches and 1.5 inches for WCDA-1
  - 20 inches and 3 inches for WCDA-2 and WCDA-3

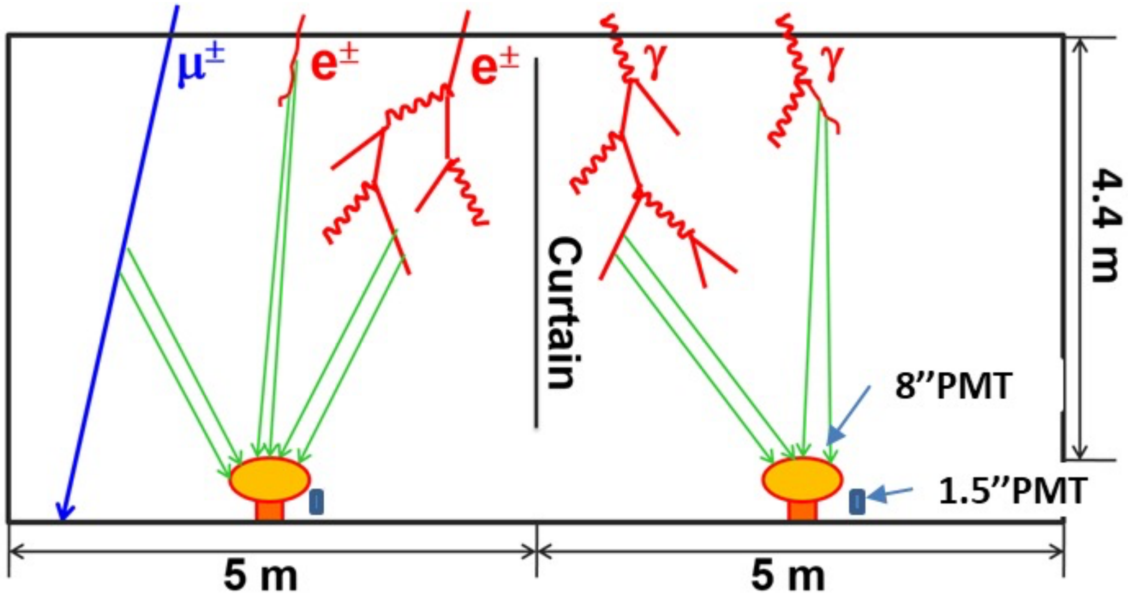

Operation of LHAASO

- KM2A is operated with >99.4% duty cycle and event rate 2×10^8 /day
- WCDA is operated with 98.4% and event rate 3×10^9 /day
- Data acquisition time of WFCTA >1400 hrs and number of matched events ~70 million

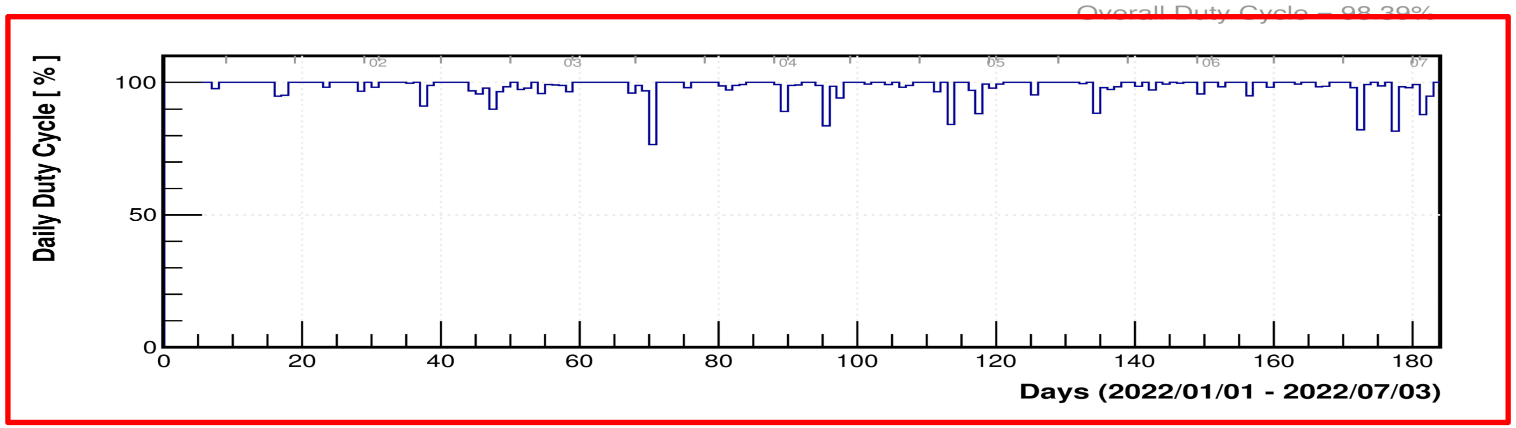

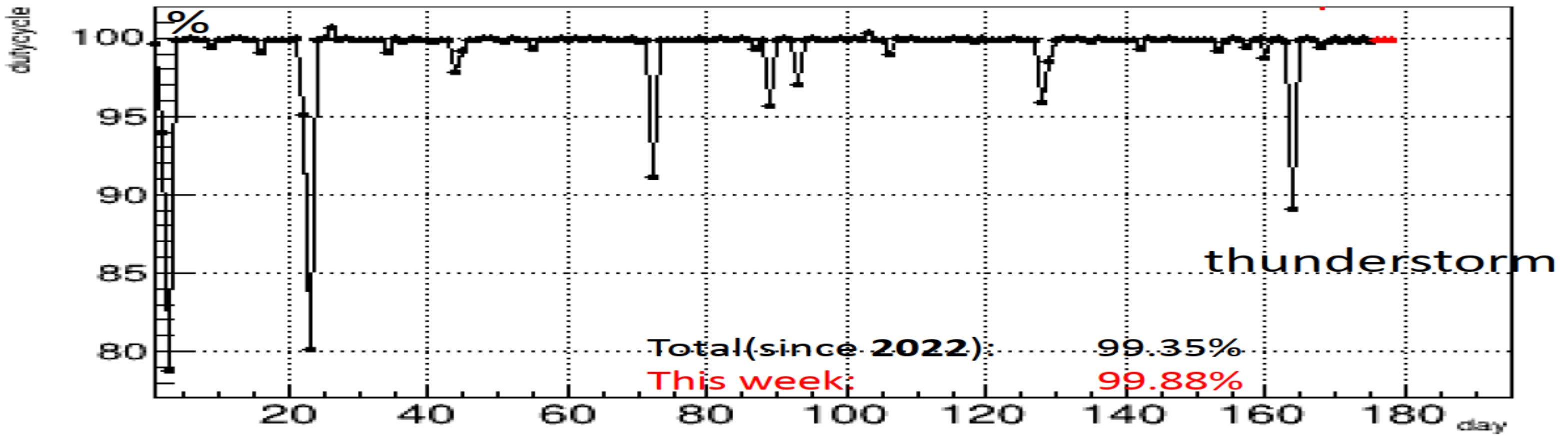

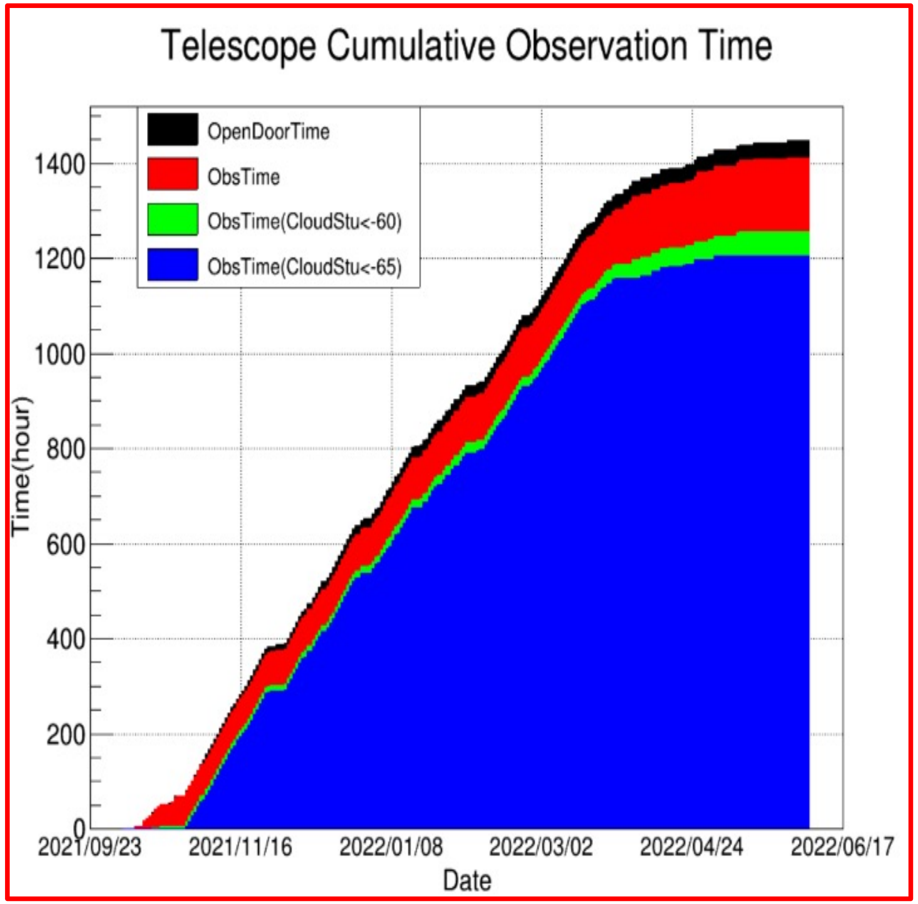

Hybrid Measurement of CR Showers around the Knee

- **WFCTA: Cherenkov telescopes**
  1. Number of pixels: Npix≥6
  2. FoV: 10° × 10° out of 16° × 16° for the centroid of the image
  3. R_p: 180 – 310 m

- **KM2A:**
  1. Core (x,y)
     - $\sqrt{x^2 + y^2} < 470\ m$
     - !|x'|<200m & !|x'|<160m
  2. Number of fired EDs > 20

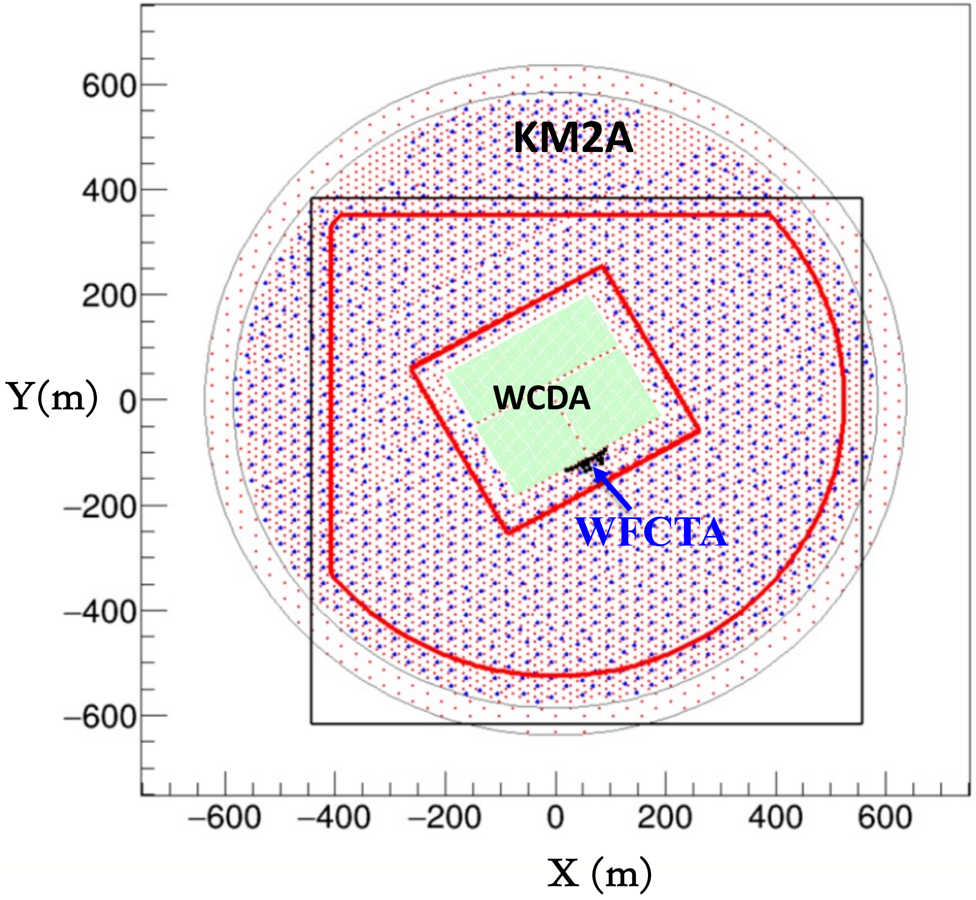

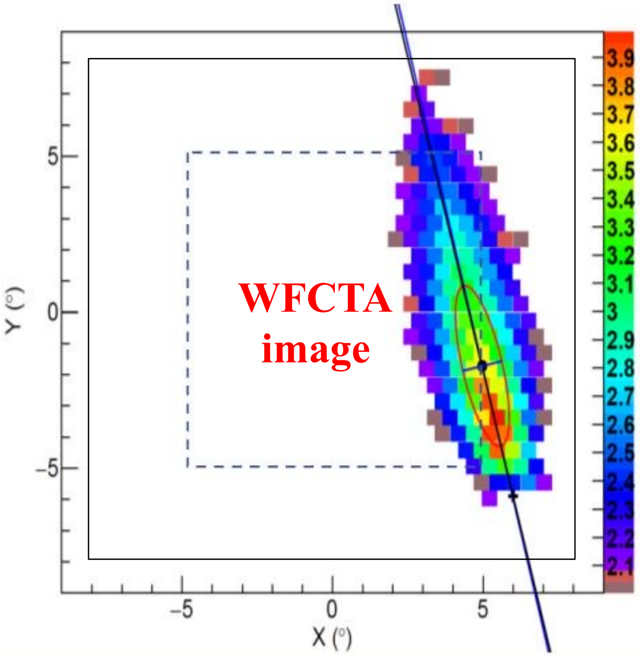

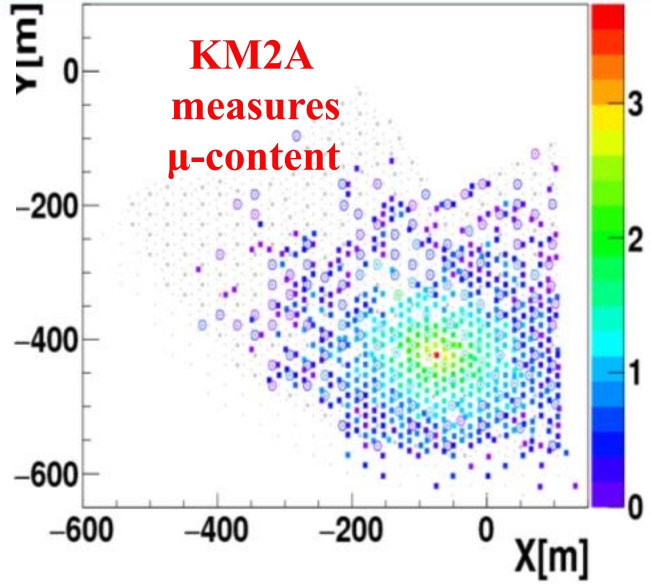

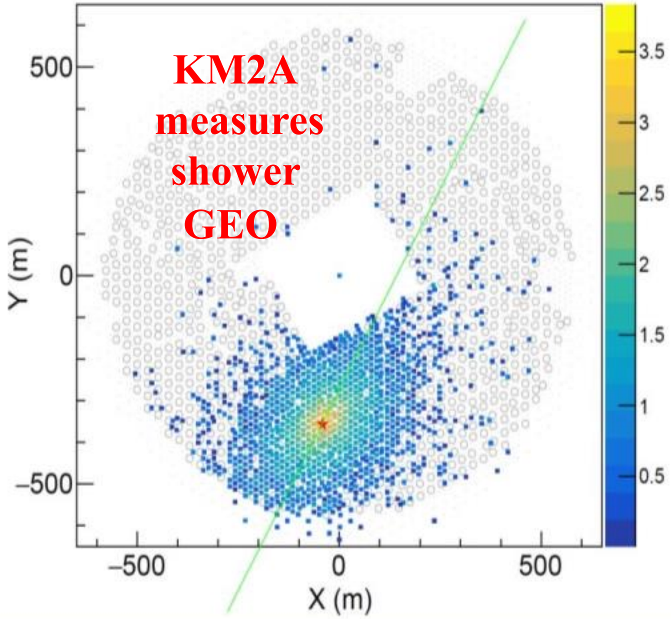

Component sensitive parameters: $P_{\mu e}$

Muons and electromagnetic particles in EAS

$$N_\mu \propto A^{1-\beta}\left(\frac{E_0}{1\ \mathrm{PeV}}\right)^{\beta} \approx 1.69\times 10^4 \cdot A^{0.10}\left(\frac{E_0}{1\ \mathrm{PeV}}\right)^{0.90}$$

$$N_e \propto A^{1-\alpha}\left(\frac{E_0}{1\ \mathrm{PeV}}\right)^{\alpha} \approx 5.95\times 10^5 \cdot A^{-0.046}\left(\frac{E_0}{1\ \mathrm{PeV}}\right)^{1.046}$$

J. R. Hörandel, Cosmic rays from the knee to the second knee: 10^{14} to 10^{18} eV, Mod. Phys. Lett. A 22, 1533 (2007)

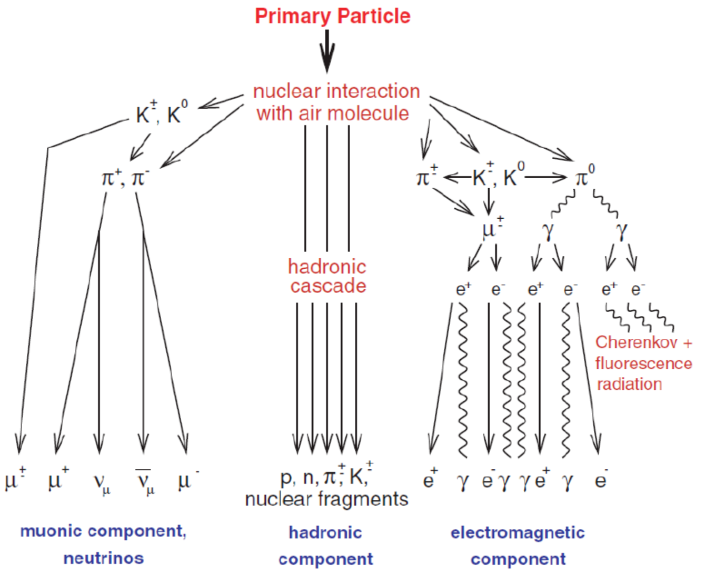

⇨ $$\log A = \frac{\alpha}{\alpha-\beta}\log\left(\frac{N_\mu}{N_e^{\beta/\alpha}}\right) + \mathrm{const}$$

$$P_{\mu e} = \log_{10}\frac{N_\mu}{N_e^{0.82}}$$

- N_μ: 40~200 m
- N_e: 40~200 m

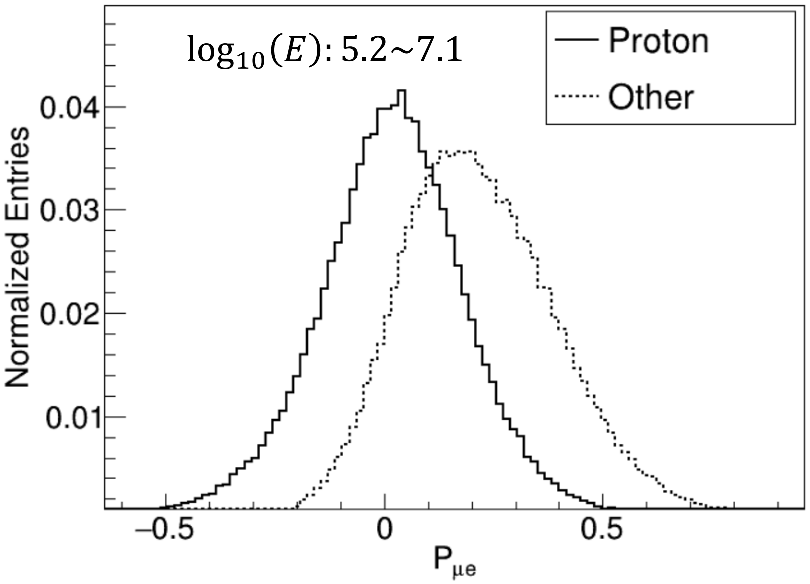

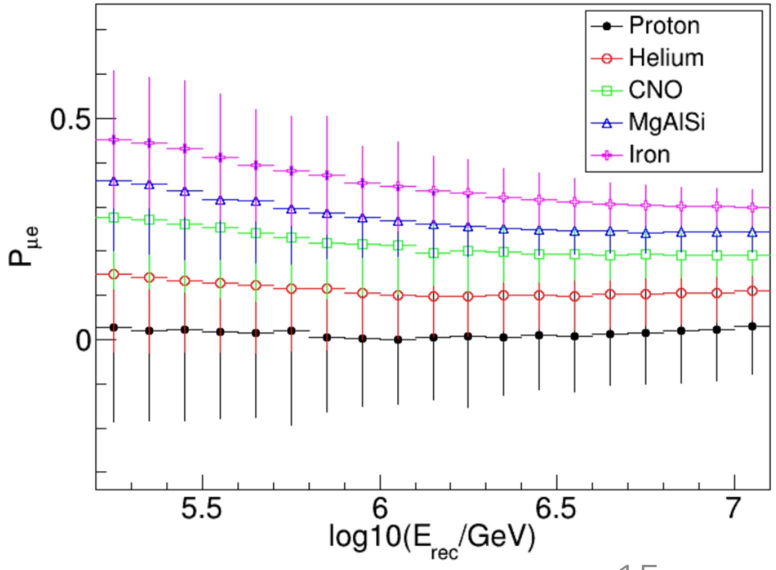

Table 1. LHAASO vs other EAS arrays

Experiment	depth g/cm^2	Detector	ΔE (eV)	e.m. Sensitive Area (m^2)	Instrumented Area (m^2)	Coverage
ARGO-YBJ	606	RPC/hybrid	$3\times10^{11}-10^{16}$	6700	11,000	0.93 (central carpet)
BASJE-MAS	550	scint./muon	$6\cdot10^{12}-3.5\cdot10^{16}$		10^4	
TIBET ASγ	606	scint./burst det.	$5\times10^{13}-10^{17}$	380	3.7×10^4	10^{-2}
CASA-MIA	860	scint./muon	$10^{14}-3.5\cdot10^{16}$	1.6×10^3	2.3×10^5	7×10^{-3}
KASCADE	1020	scint./mu/had	$10^{15}-10^{17}$	5×10^2	4×10^4	
KASCADE -Grande	1020	scint./mu/had	$10^{16}-10^{18}$	370	5×10^5	7×10^{-4}
Tunka	900	open Cher.det.	$3\cdot10^{15}-3\cdot10^{18}$	-	10^6	-
IceTop	680	ice Cher.det.	$10^{15}-10^{18}$	4.2×10^2	10^6	4×10^{-4}
LHAASO	600	Water C scint./mu/had Wide FoV Cher.Tel	$3\times10^{11}-10^{18}$	5.2×10^3	1.3×10^6	4×10^{-3} [KM2A]

Muon detectors

Experiment	m asl	μ Sensitive Area [m^2]	Instrumented Area [m^2]	Coverage
LHAASO	4410	4.2×10^4	10^6	4.4×10^{-2}
TIBET ASγ	4300	4.5×10^3	3.7×10^4	1.2×10^{-1}
KASCADE	110	6×10^2	4×10^4	1.5×10^{-2}
CASA-MIA	1450	2.5×10^3	2.3×10^5	1.1×10^{-2}

Component sensitive parameters: $P_{\theta c}$

X_{max} in EAS

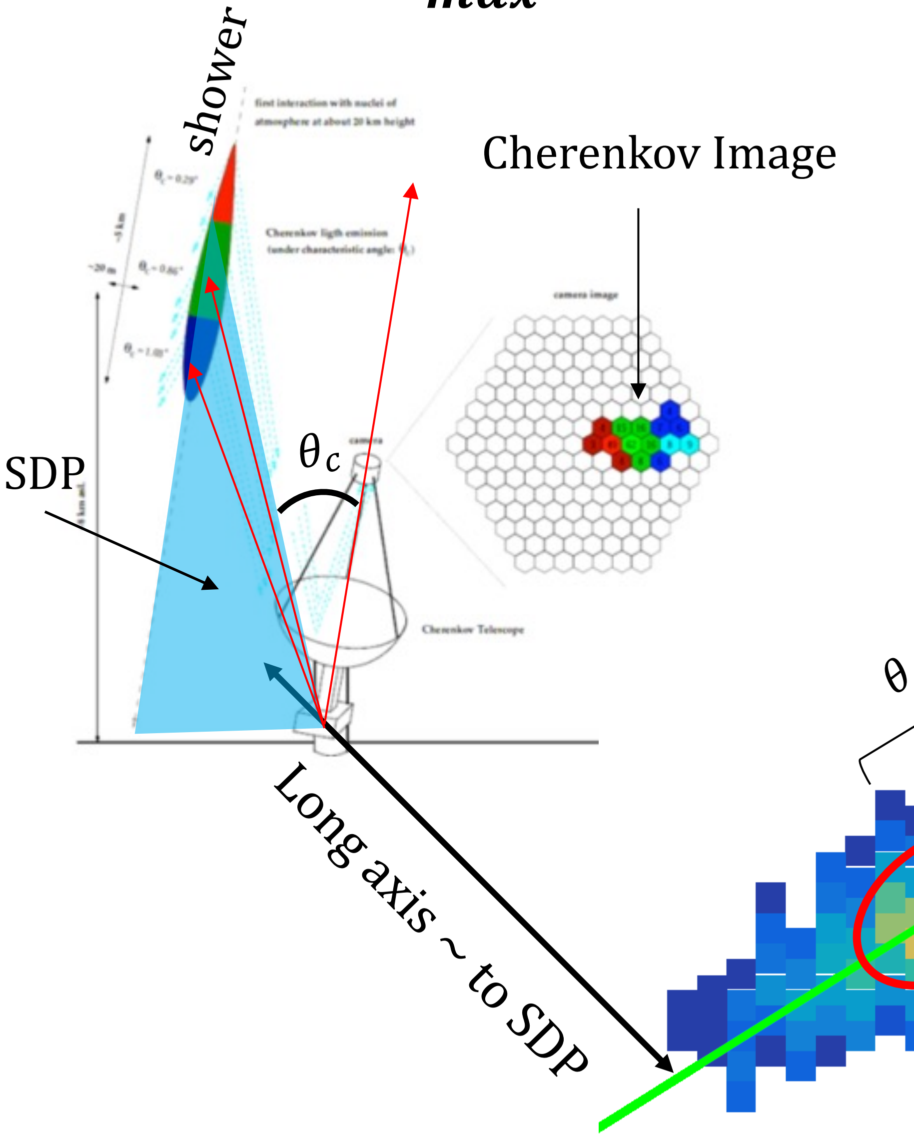

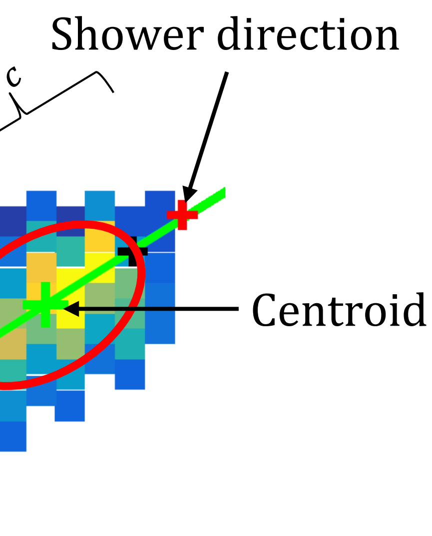

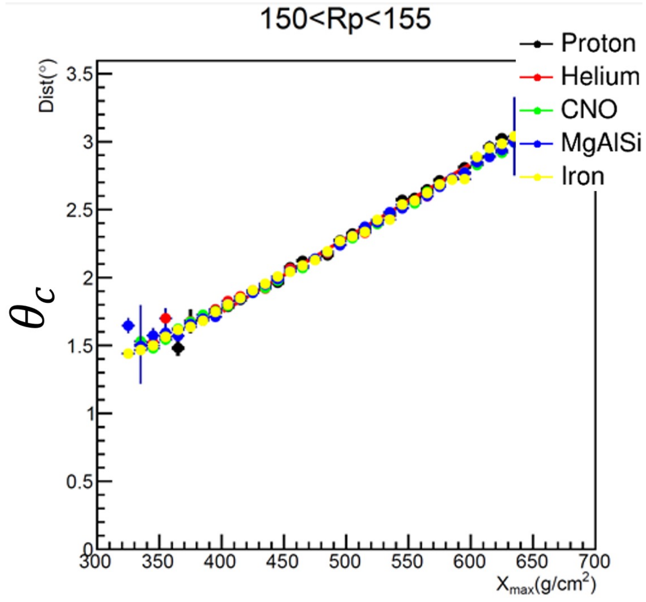

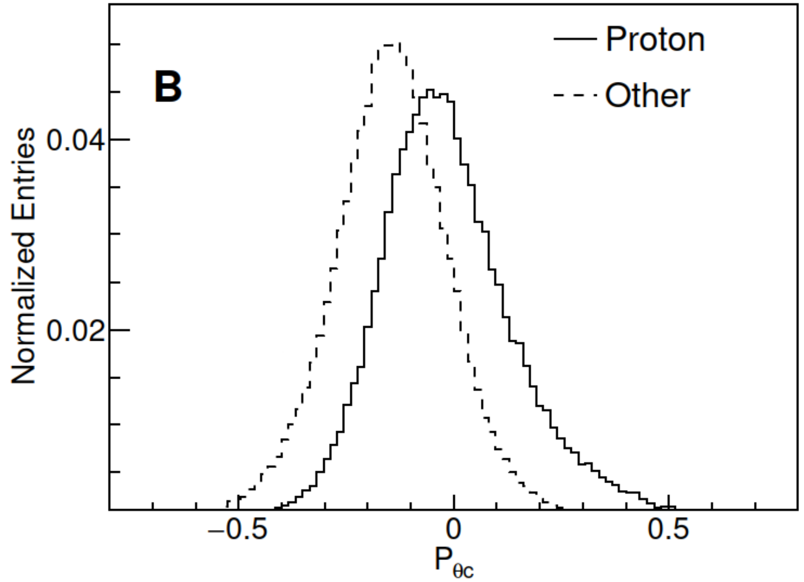

$$P_{\theta c} = \frac{\theta_c^{250} - \langle\theta_c^{250}\rangle}{\langle\theta_c^{250}\rangle|_{PeV}}$$

- Normalization in the impact parameter R_p:

$$\theta_c^{250} = \frac{\theta_c}{\cos(\theta)} + 0.011\times(R_p - 250)$$

- Normalization in energy:

$$\langle\theta_c^{250}\rangle = p_0 + p_1 \cdot \log_{10} E + p_2 \cdot \log_{10}^2 E$$

- $\langle\theta_c^{250}\rangle|_{PeV}$: the average value of θ_c for proton events at R_p =250 m and E=1 PeV

Proton Selection

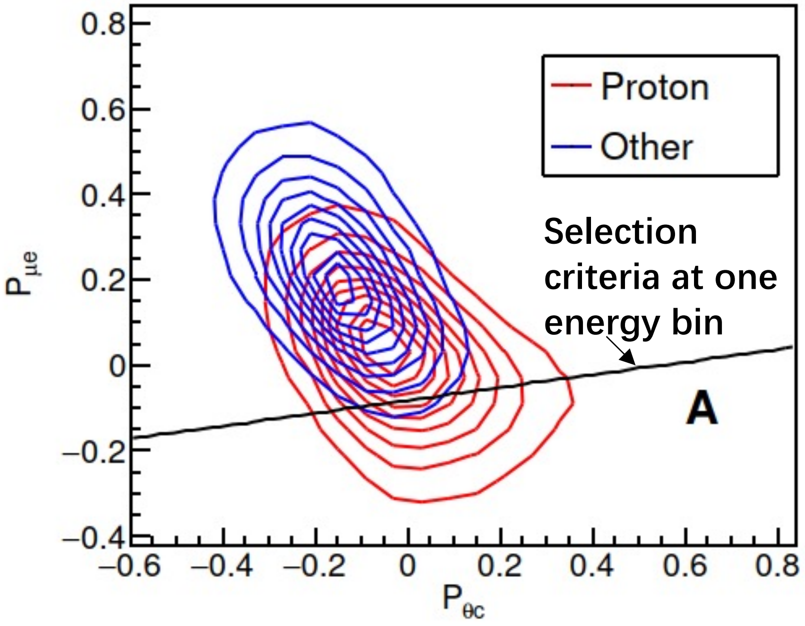

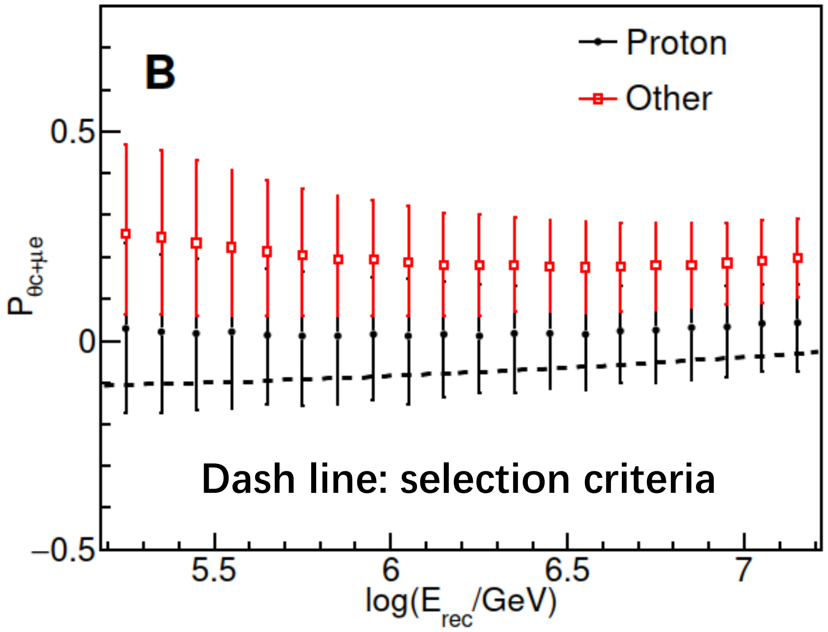

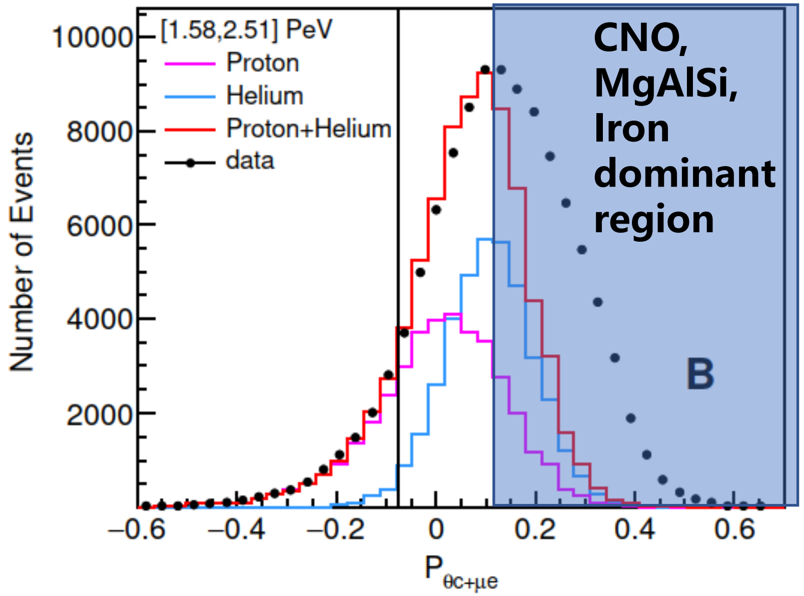

$$P_{\theta c+\mu e} = -\sin(\delta)\cdot P_{\theta c} + \cos(\delta)\cdot P_{\mu e} \quad (\delta = 8.5^\circ)$$

- Purity ($\epsilon^l = \frac{N^L_{select}}{N^L_{select}+N^H_{select}}$) : ~90% @ 1PeV
  - Most of the contaminations come from Helium
- Selection efficiency ($\eta^l = \frac{N^L_{select}}{N^L_{all}}$) : 25%.

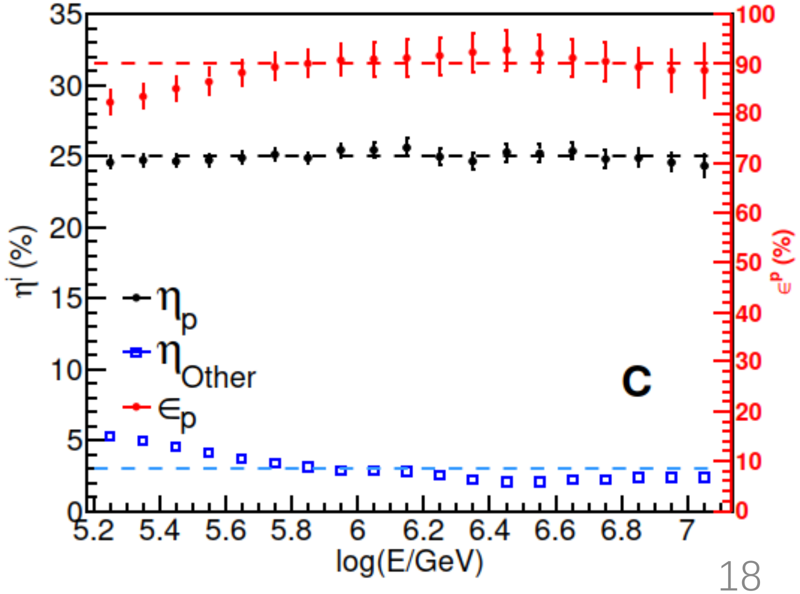

Energy Reconstruction

- **Shower energy: $E_0 = E_{em} + E_h$**
  - Electromagnetic component (E_{em}): Cherenkov photons (N_{ph}) or $electrons + gamma$ rays (N_e)
  - $Hadronic\ component$(Eh): $\pi^{\pm} \rightarrow \mu$ （N_{μ}）

$$N_{c\mu} = N_{ph} + CN_u$$
$$E_{rec} = kN_{c\mu}$$

- Energy Resolution： <15%
- Systematic Bias： <2%

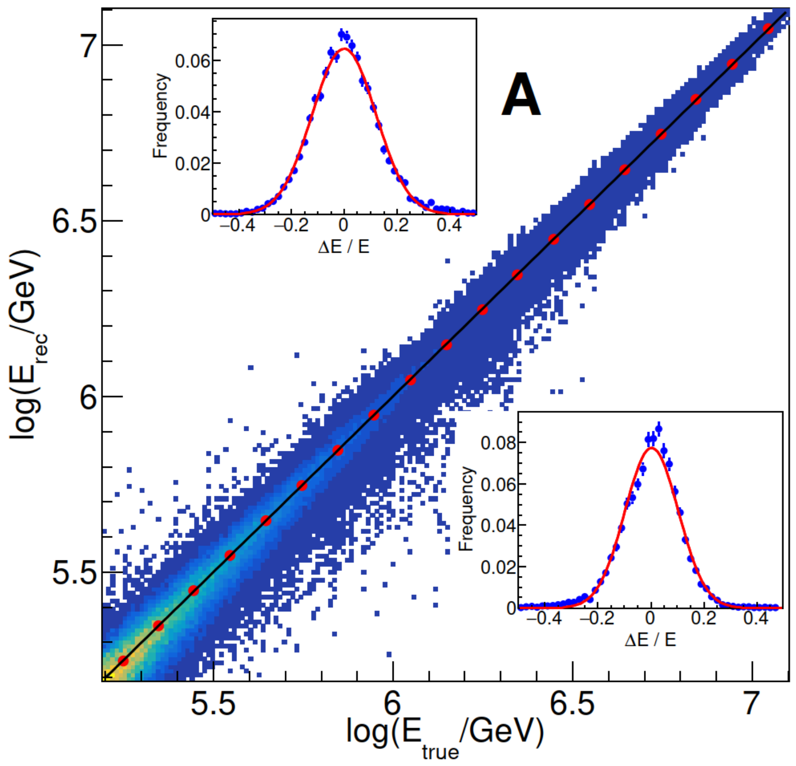

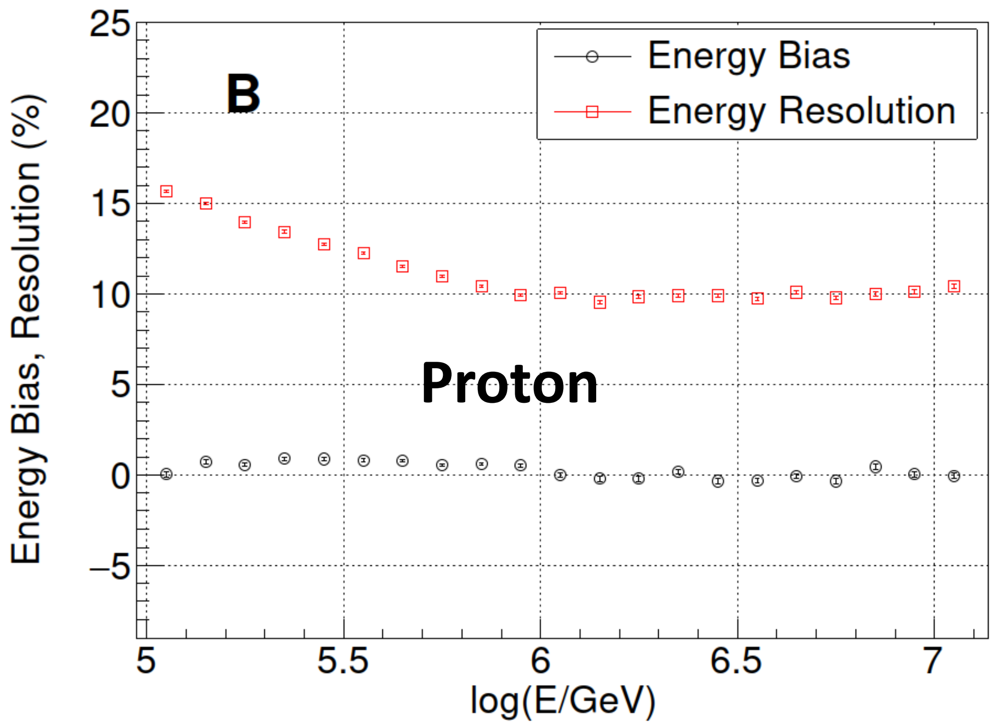

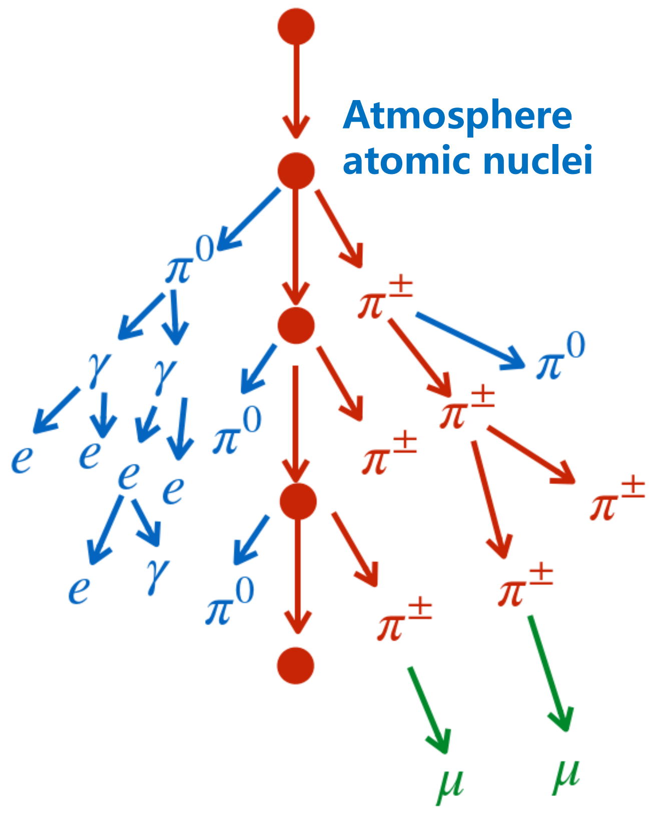

Proton energy spectrum measured by LHAASO in the knee region

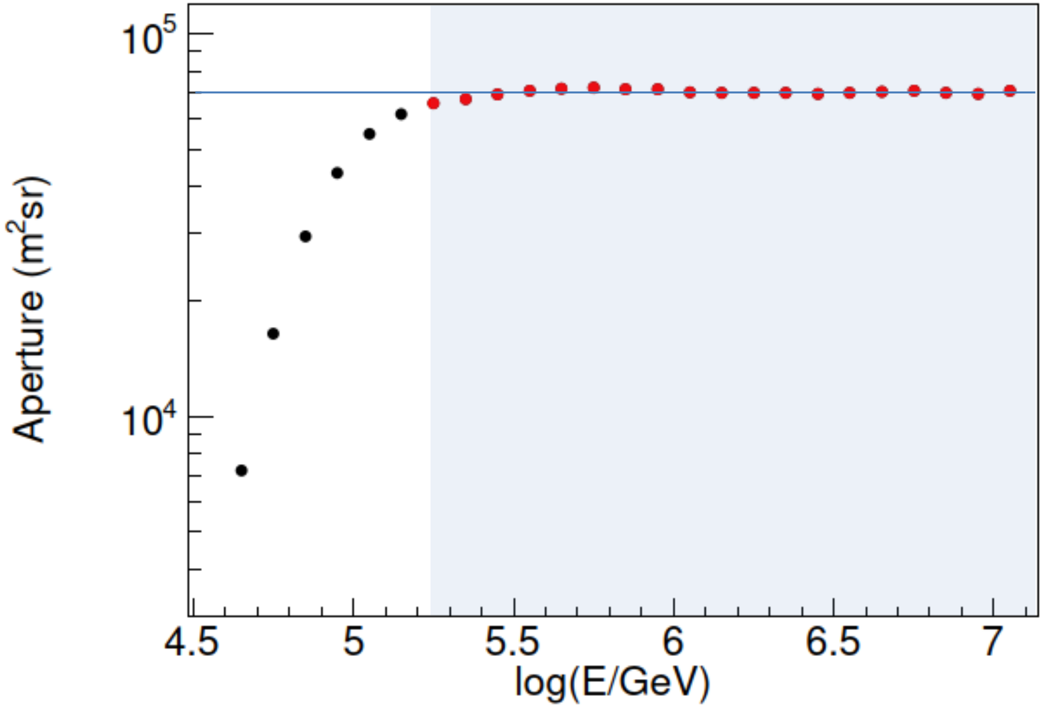

LHAASO Coll., arXiv:2505.14447

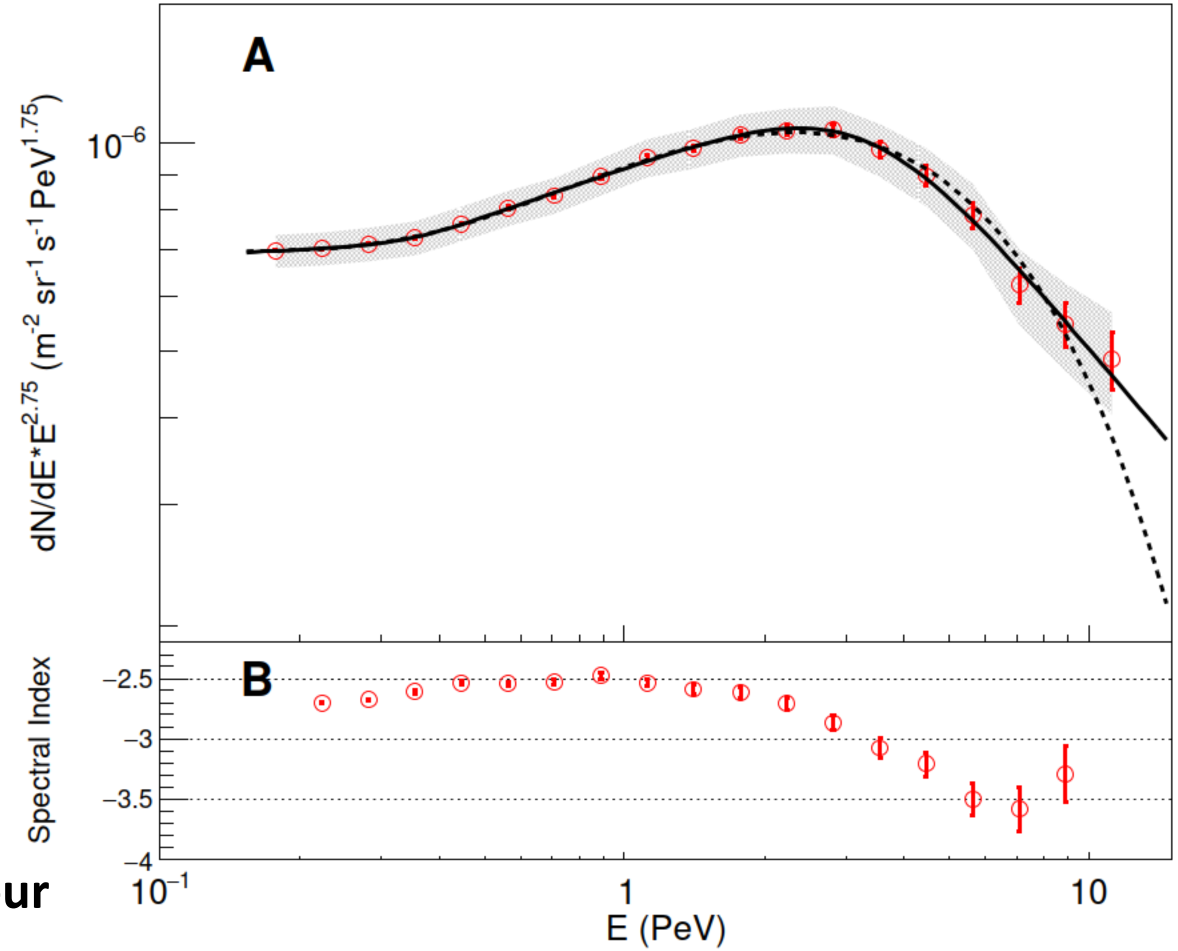

- **Data set： 2021.10-2022.4**
- **Total time after good weather selection: ~1,000 hour**
- **Aperture: ~70,000 m^2sr**
- **The proton energy spectra from 158TeV to 12.5 PeV were measured with high precision by LHAASO**

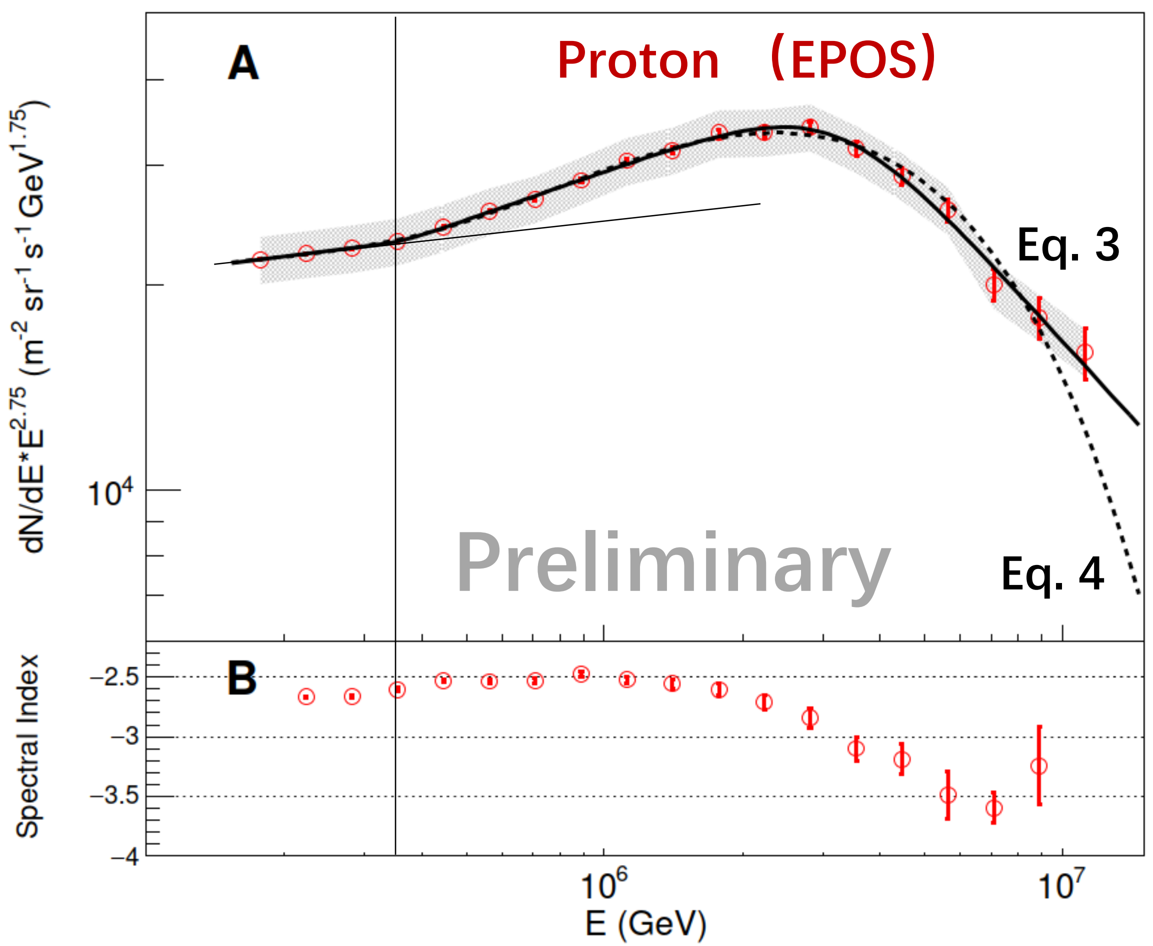

- Eq. 3： Two broken power laws

E_h = 365 ± 20
E_k = 3.2±0.3
γ1 = −2.67± 0.01
γ2 = −2.51±0.02
γ3 = −3.5±0.1
χ^2/n.d.f. = 9.9/11

- Eq. 4： A broken power law + an exponential cutoff

E_h = 436 ± 22
E_{cut} = 5.1 ± 0.3
γ1 = −2.66 ± 0.02
γ2 = −2.29 ± 0.05
χ^2/n.d.f. = 27.1/13

Eq. 3： $$F(E) = F_0 \left(\frac{E}{100TeV}\right)^{\gamma_1} \left(1 + \left(\frac{E}{E_h}\right)^{1/w_1}\right)^{(\gamma_2-\gamma_1)w_1} \left(1 + \left(\frac{E}{E_k}\right)^{1/w_2}\right)^{(\gamma_3-\gamma_2)w_2}$$

Eq. 4： $$F(E) = F_0 \left(\frac{E}{100TeV}\right)^{\gamma_1} \left(1 + \left(\frac{E}{E_h}\right)^{1/w}\right)^{(\gamma_2-\gamma_1)w} e^{-\frac{E}{E_{cut}}}$$

Proton energy spectrum measured by LHAASO in the knee region

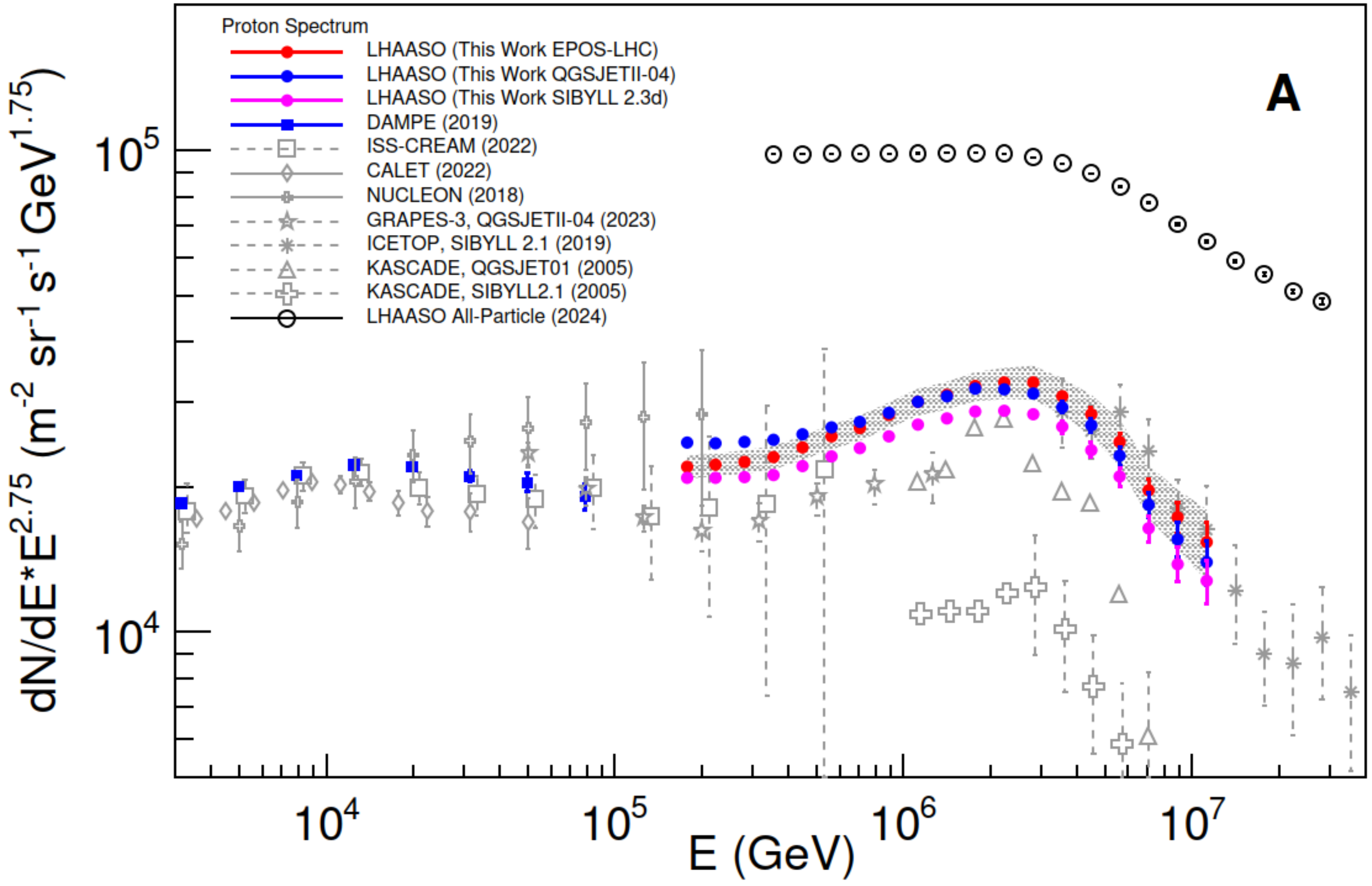

LHAASO Coll., arXiv:2505.14447

- CR protons around the knee have been identified with high purity for the first time, and their energy spectrum has been precisely measured from 0.15 to 12 PeV by LHAASO.
  - LHAASO purity: ~90%, above 100TeV
  - Direct measurement (e.g. DAMPE) purity: 99% - 95%, below 100TeV
  - KASCADE and ICETOP: Unfolding method, no purity provided.
- Hardening: ~340 TeV, with index change $\Delta\gamma$=~0.2
- Softening (knee): ~3.3 PeV, with index change $\Delta\gamma$=~−1

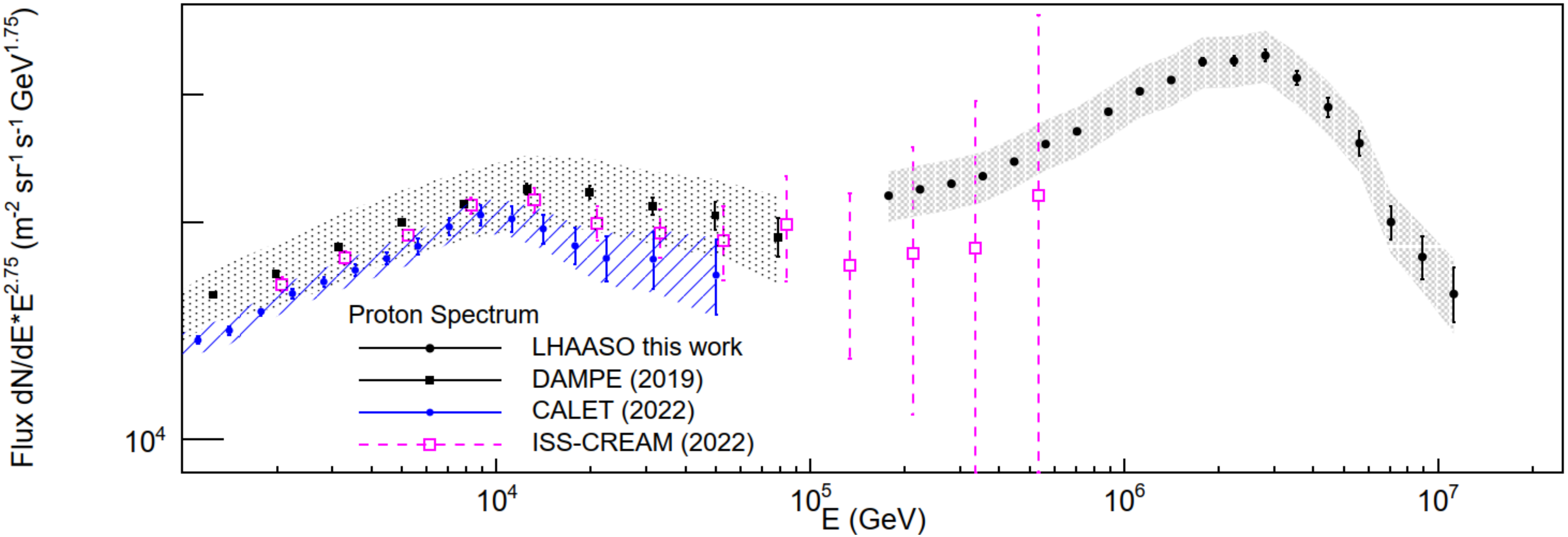

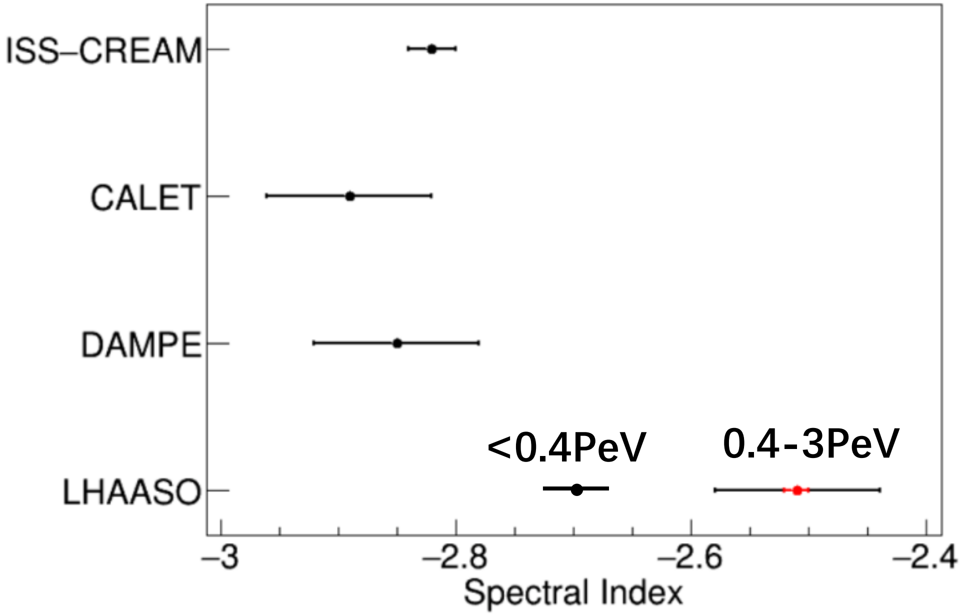

- **A hardening feature is found bellow the knee.**
- **The direct measurement results such as DAMPE, CALET, ISS-CREAM, further confirm the existence of the hardening before the knee.**

Proton knee vs. all particle knee

LHAASO Collaboration, PRL, 132, 131002 (2024)

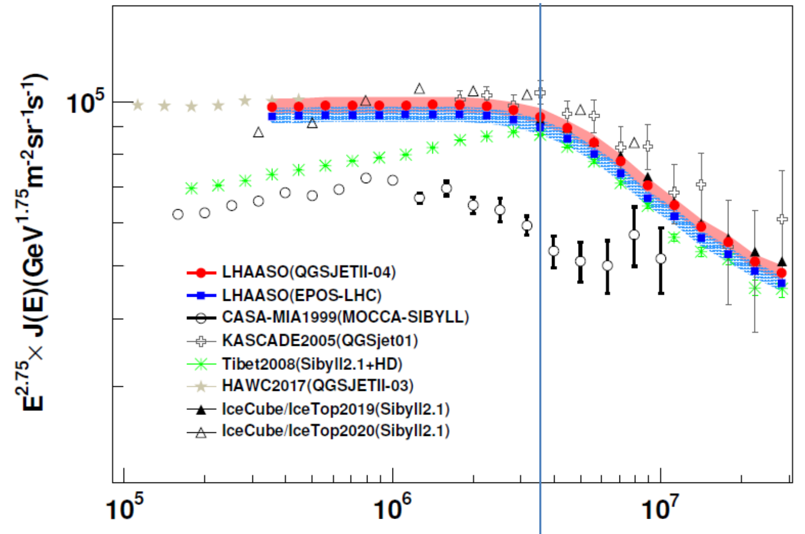

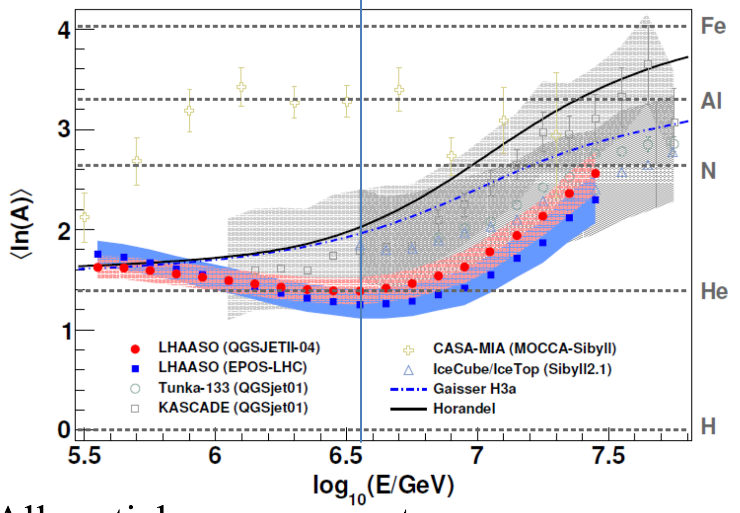

All particle energy spectrum: see Hengying Zhang talk for more details.

Knee: ~3.67 PeV
γ1 = -2.74±0.005
γ2 = -3.13±0.005

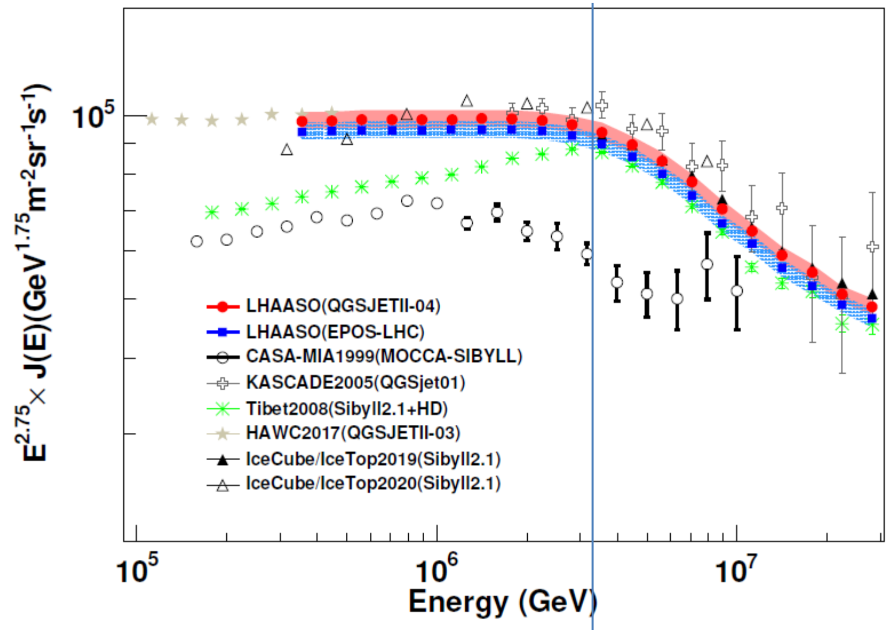

Knee: ~3.3 PeV
γ1 = −2.71 ± 0.02
γ2 = −2.51 ± 0.03
γ3 = −3.5 ± 0.2

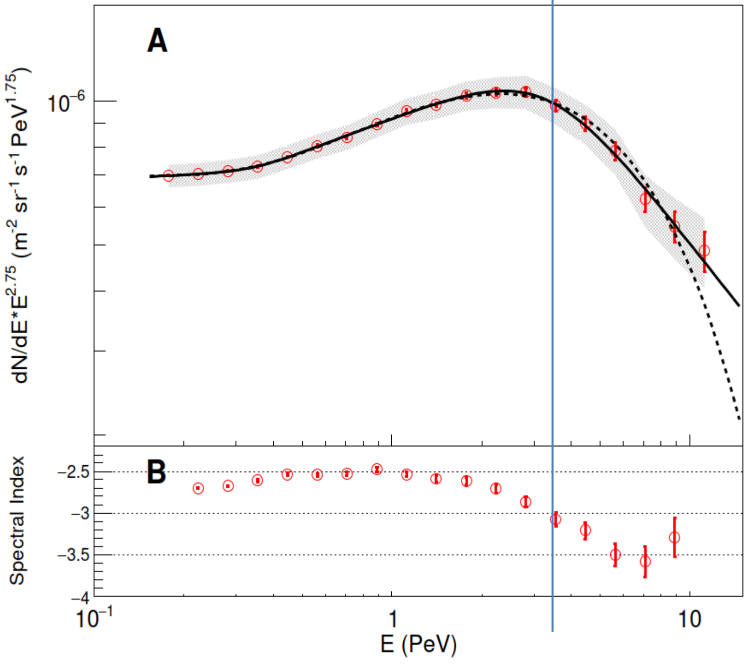

The all-particle knee is likely dominate by the proton knee.

- 首次在观测上确认全粒子能谱的膝结构（3.67PeV）是由质子的拐折导致的

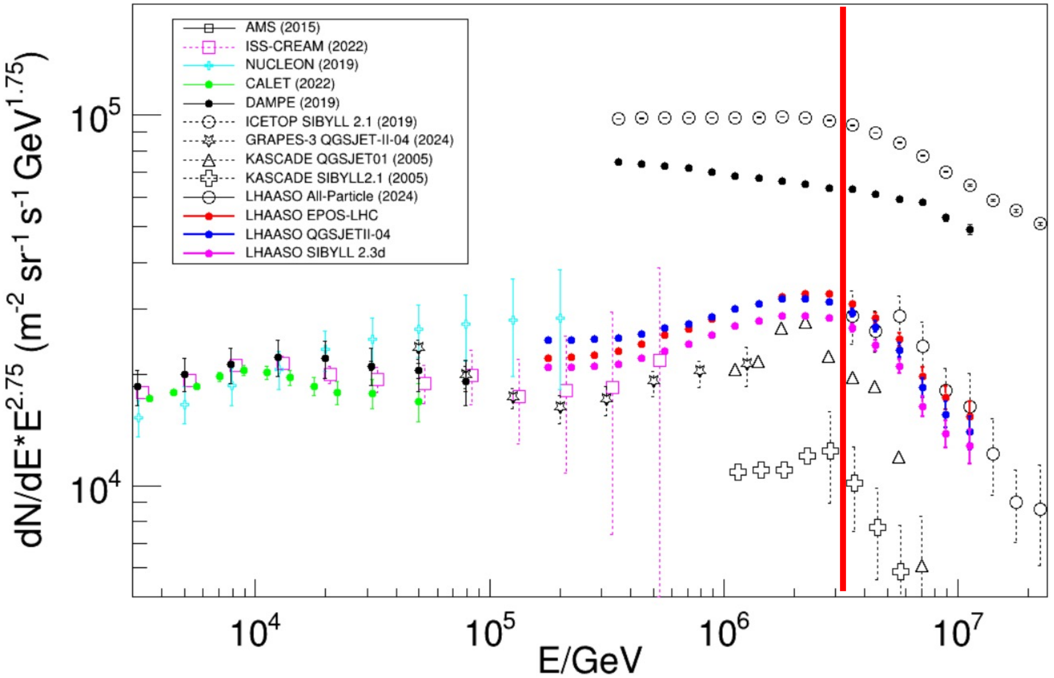

全粒子能谱减去质子能谱

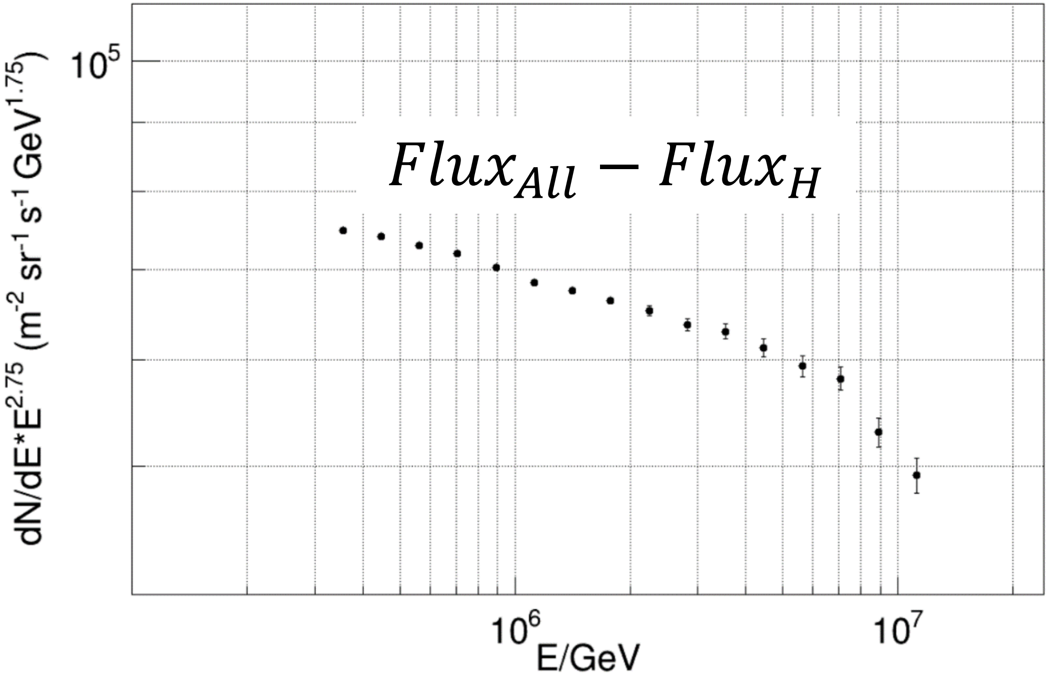

质子能谱文章已经被国际同行引用超过8次，在今年的国际宇宙线大会上也受到热烈关注

Wideband spectrum of protons

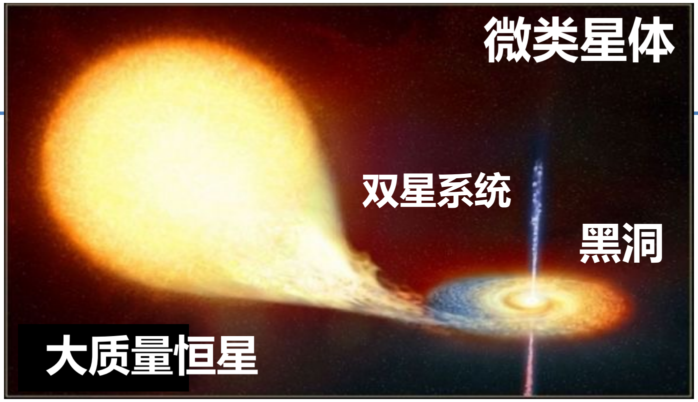

- A potential explanation could be the existence of multiple groups of cosmic ray sources with varying acceleration limits, as indicated by their maximal cosmic ray energies.

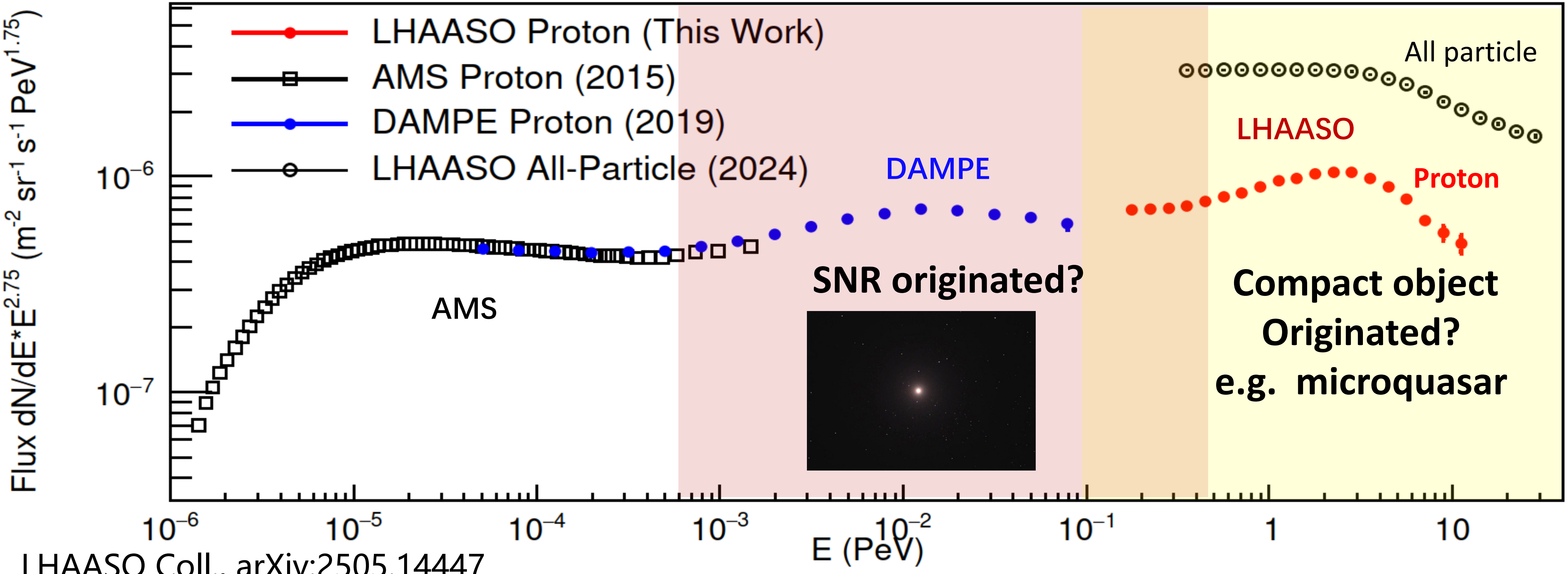

LHAASO Coll., arXiv:2505.14447

Systematic Uncertainties

Systematic uncertainties on flux	
Hadronic model	≤ 15%
Composition model	~7%@3PeV
Different purity	≤ 2%
SiPM camera calibration	≤ 2%
Background light	≤ 2%
Absolute Humidity	≤ 1%
Air pressure	≤ 1%
Total	~17 %

Systematic uncertainties on Energy Scale	
SiPM camera calibration	~1.5%
Mirror reflectivity Calibration	~1%
Nμ Calibration	~1%
Absolute Humidity (water vapor)	~1%
Aerosol	~2%
Air pressure	~0.5%
Hadronic model	~1.4%
Total	~4%

宇宙线绝对能标研究计划

➢ **To understand the absolute energy scale of cosmic rays, a joint analysis by LHAASO and DUMPE is in progress and is expected to be completed by the end of this year.**

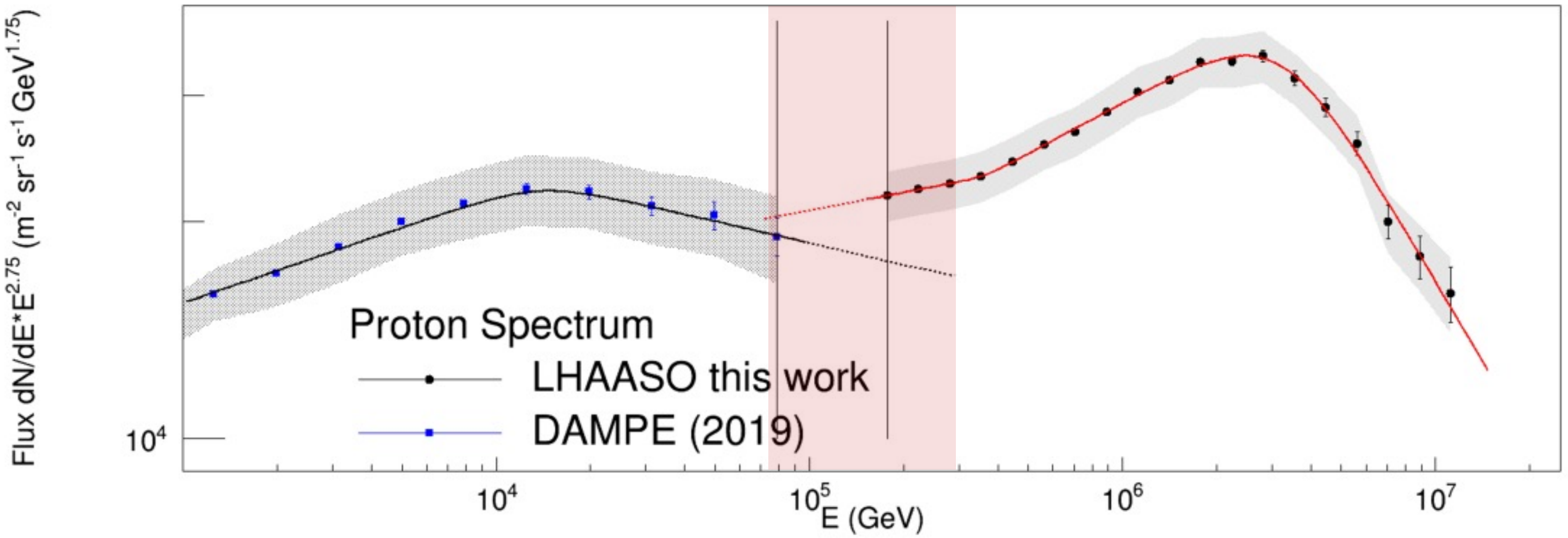

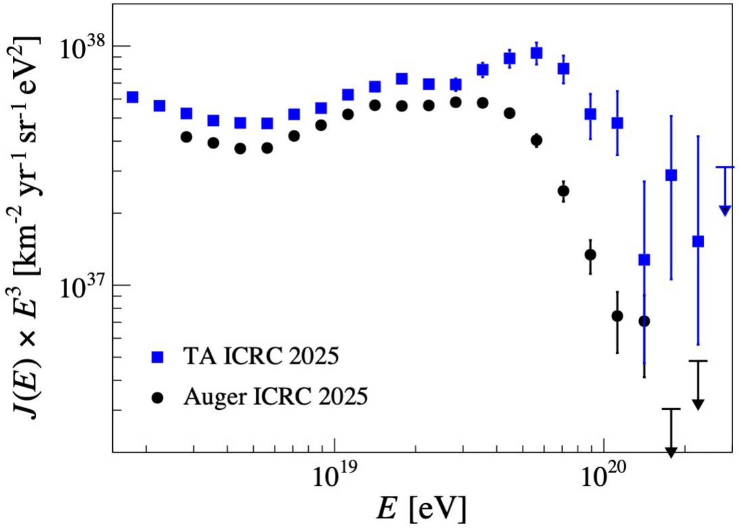

Outline

- Introduction
- Proton energy spectrum measurement results in the knee region
- **All particle energy spectrum and mass**
- Progress in the helium energy spectrum
- Summary & Outlook

Analysis and Result

KM2A full array simulation data

- QGSJETII-04_fluka and EPOS-LHC_fluka
- Proton He CNO MgAlSi Fe
- Theta:0-40°
- Slope: -2
- Sample Radius： 200-480m

Event Selection:

θ: 22-38° (X_{max}: 650-760 g/cm^2)
$\Omega = 0.75$ sr
R: 300-450m
Aperture=2.65e5 m^{2}sr
Ne: >100

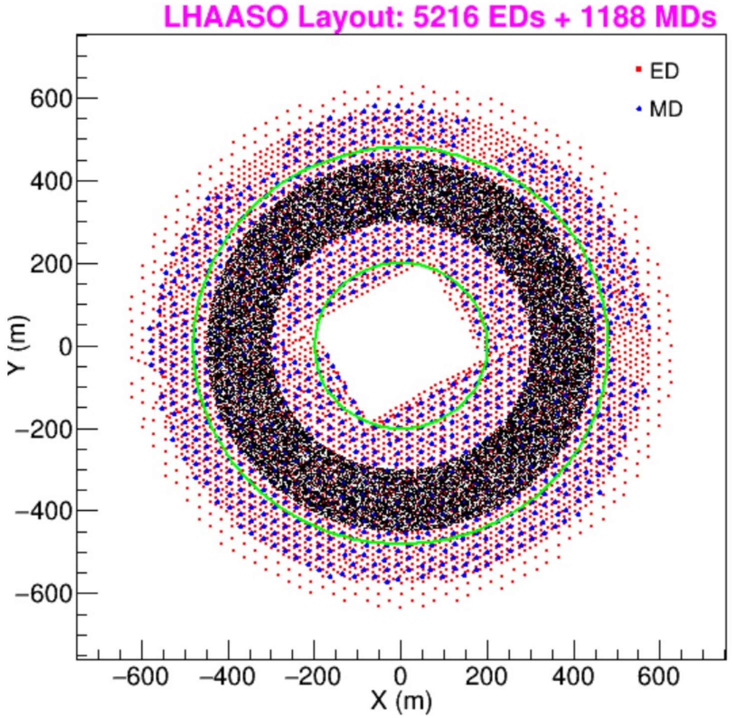

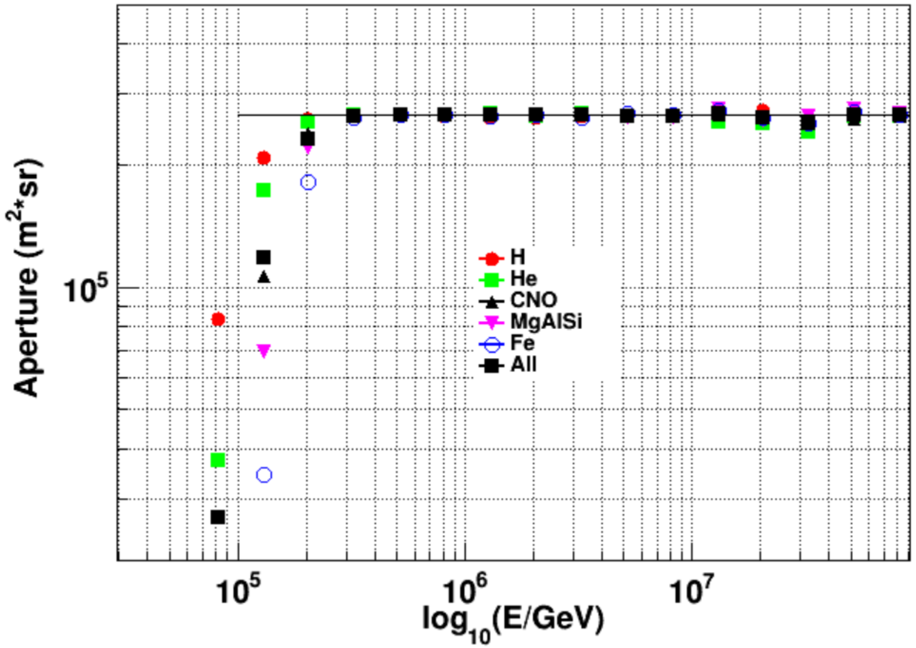

Analysis and Result

Energy reconstruction

As Heitler's EM model and Matthews' hadronic showers model introduced that the primary energy is finally divided between pions and electromagnetic particles in sub-showers.

$$E_0 = E_e + E_h \qquad E = 0.85GeV(N_e + 25 * N_\mu)$$

J. Matthews Astroparticle Physics 22 (2005) 387–397

one combined variable to reconstruct the cosmic ray energy weakly dependent on the components

$$N_{e\mu} = N_e + 2.8 * N_\mu$$

H.Y. Zhang, H.H. He and C.F. Feng PRD 106, 123028 (2022)

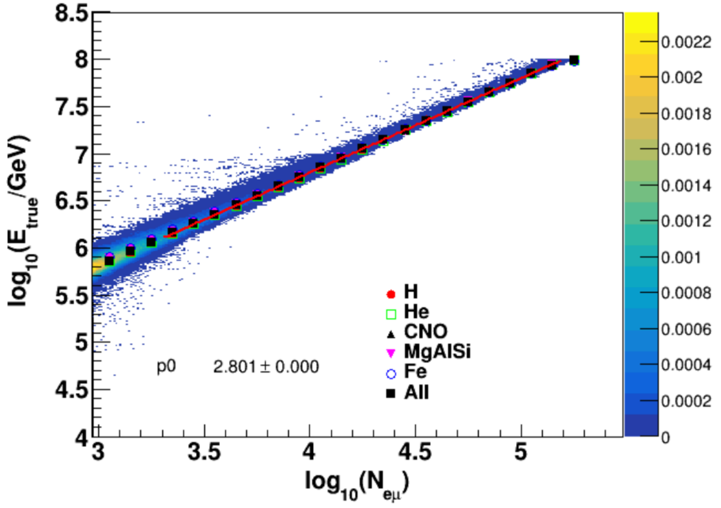

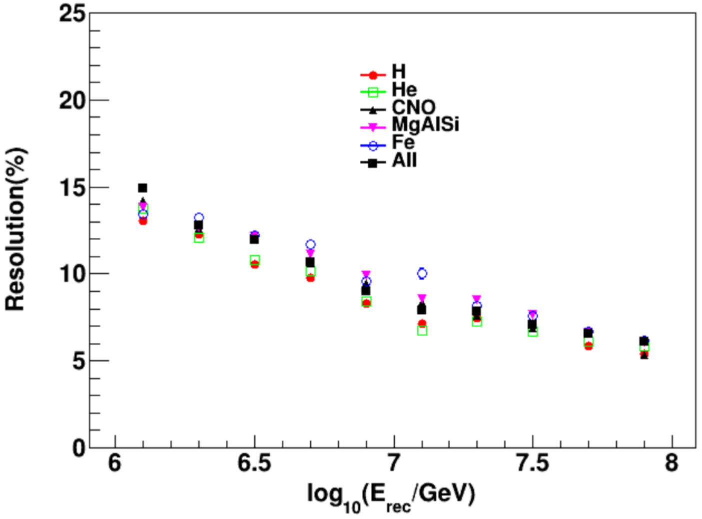

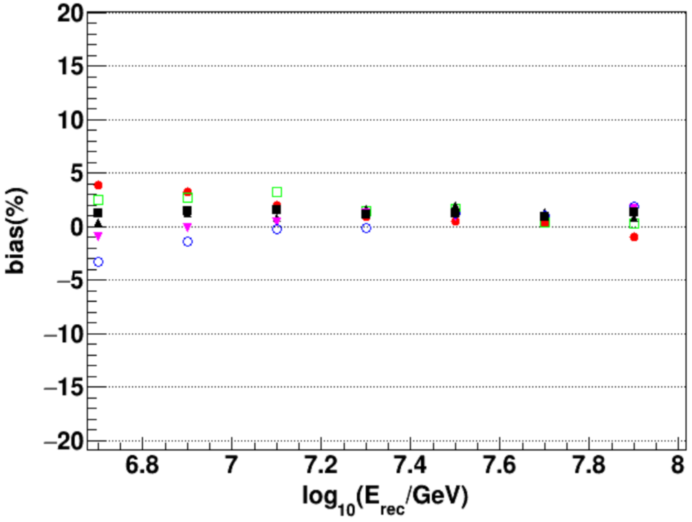

Analysis and Result

② All-Particle Energy Spectrum of cosmic ray

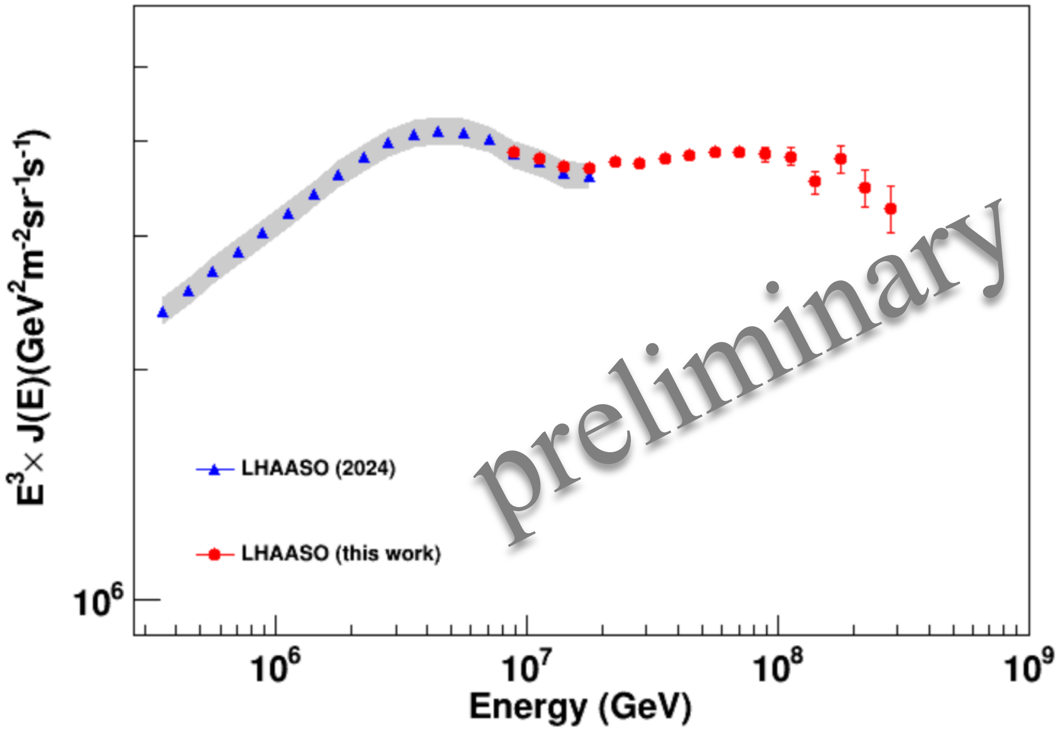

$$flux = \frac{\Delta N}{\Delta E * Aperture * T}$$

$$stat.\,err = \frac{\sqrt{\Delta N}}{\Delta E * Aperture * T}$$

Red dot: 2021.09-2024.06 data measured all-particle energy spectrum of cosmic ray

Analysis and Result

③ Measurement of muon content

Muons are the direct messengers of the hadronic processes occurring in the shower. The number of muon is a sensitive parameter to study the composition of cosmic rays and test hadronic interaction model.

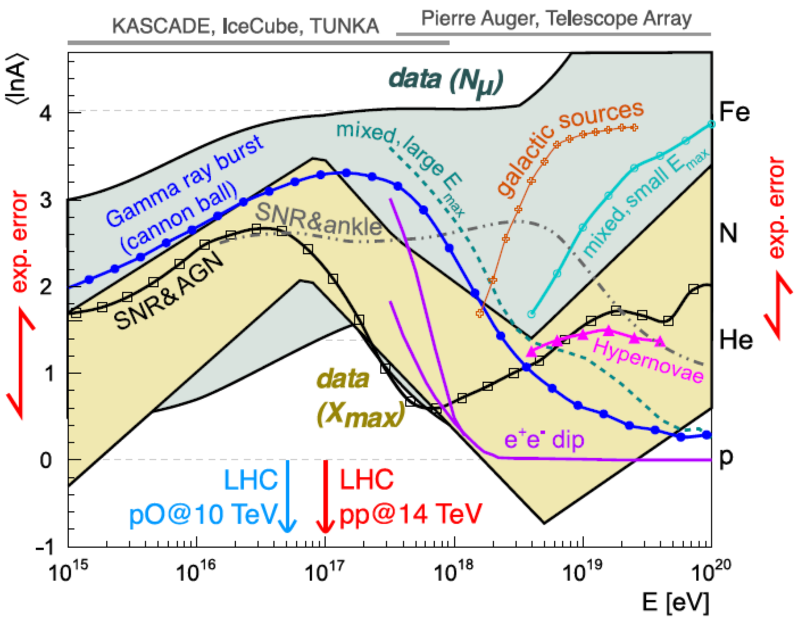

EPJ Web Conf. 210 (2019) 02004

$$N_\mu = A\left(\frac{E/A}{\varepsilon_C}\right)^\beta$$

muon number depends on cosmic ray energy and mass A

$$\langle \ln N_\mu \rangle = x_0 + x_1 \langle \ln A \rangle$$

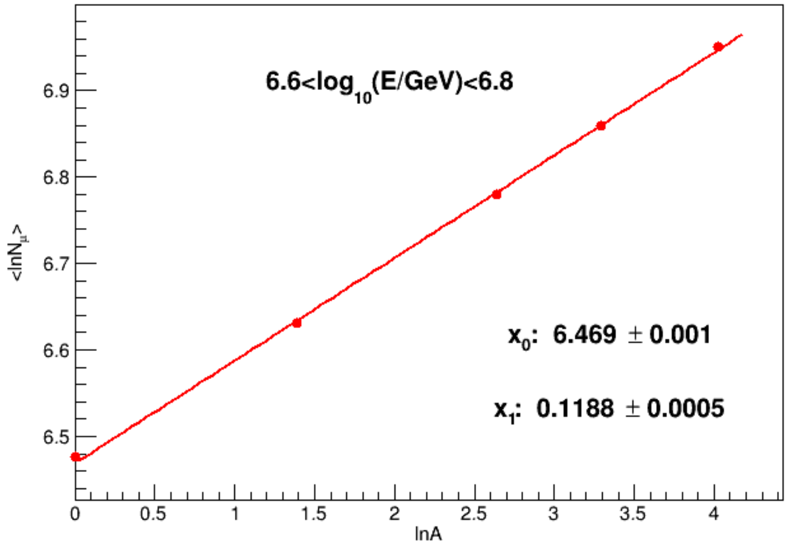

$$x_0 = \langle \ln N_\mu \rangle_H$$

$$x_1 = 1 - \beta$$

Analysis and Result

⑤ Mean logarithmic mass ⟨ln A⟩ of cosmic rays

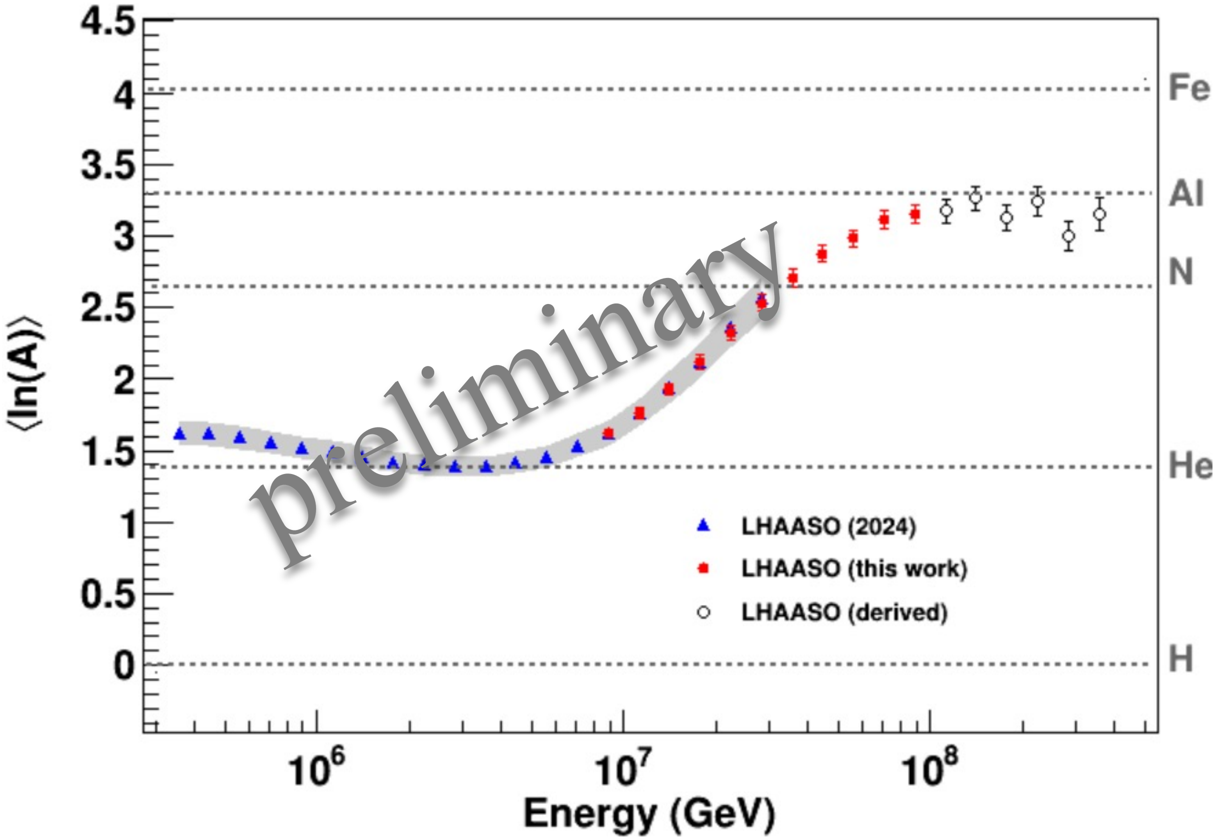

Red dot: 2021.09-2024.06 data measured mean logarithmic mass ⟨ln A⟩ of cosmic rays

- Above "knee" region, the cosmic ray component becomes heavier and then flattens at 100 PeV and shows a decreasing trend with increasing energy, suggesting that the cut-off of the all-particle energy spectrum is heavy components.

Outline

- Introduction
- Proton energy spectrum measurement results in the knee region
- All particle energy spectrum and mass
- **Progress in the helium energy spectrum**
- Summary & Outlook

Summary & Outlook

- CR protons around the knee have been identified with high purity for the first time, and their energy spectrum has been precisely measured from 0.15 to 12 PeV by LHAASO
  - **Uncovering the proton 'knee' around 3.3 PeV and a hardening feature at around 0.34 PeV.**
  - **Measuring CR Spectra of individual species around knees is a big step towards understanding the knee feature and its origin.**
- **To understand the absolute energy scale of cosmic rays, a joint analysis by LHAASO and DUMPE is in progress and is expected to be completed by the end of this year.**
- **The paper of light component and helium energy spectra will be ready soon.**
- **The iron spectrum around 400 TeV will be finished next year and iron spectrum around the knee is the goal in 3 years.**

未来计划：更高能量的分成分能谱测量

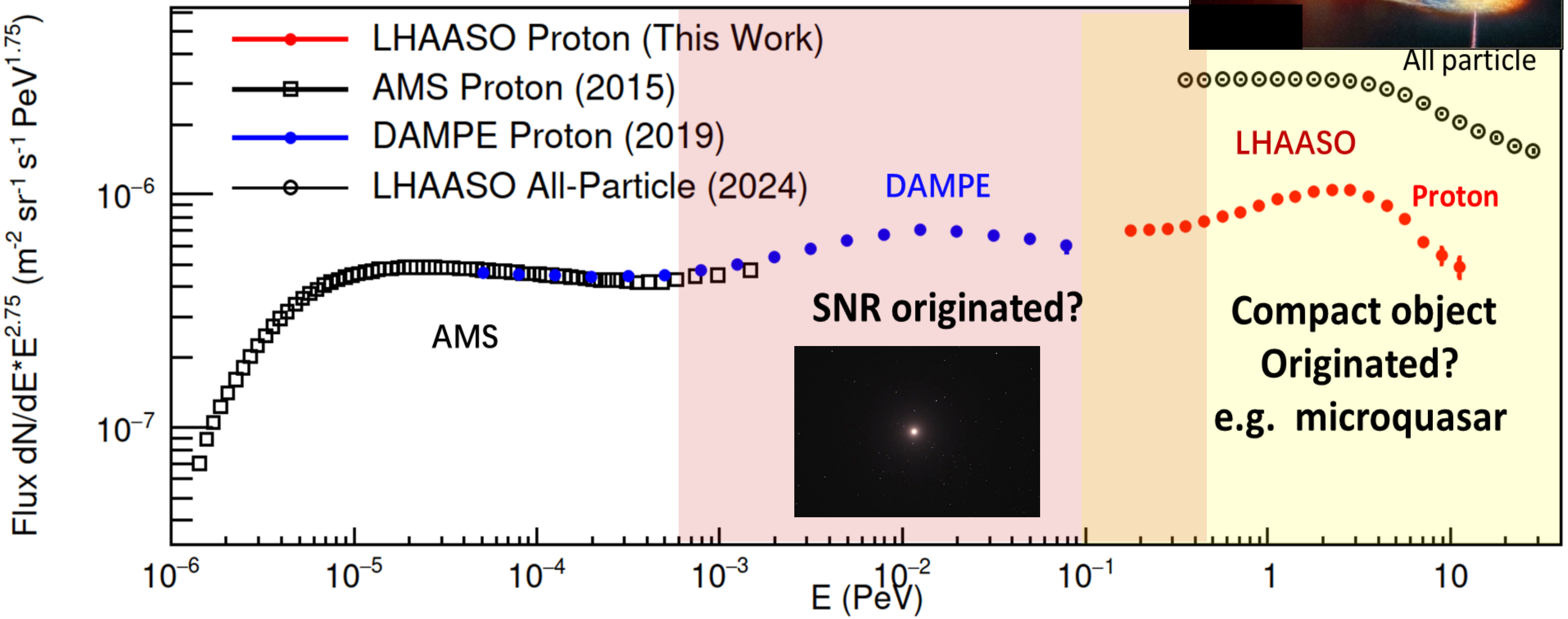

更高能量

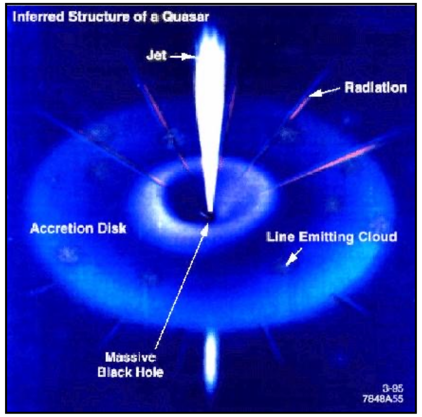

活动星系核：超大质量黑洞

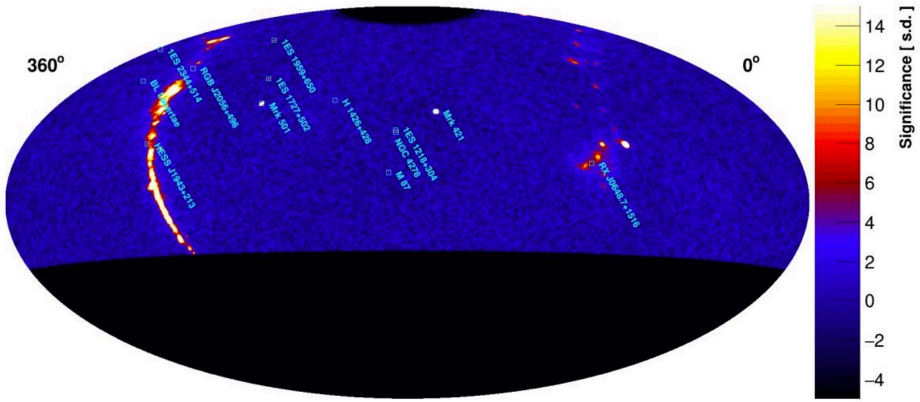

目前已经探测到的河外TeV辐射源天图

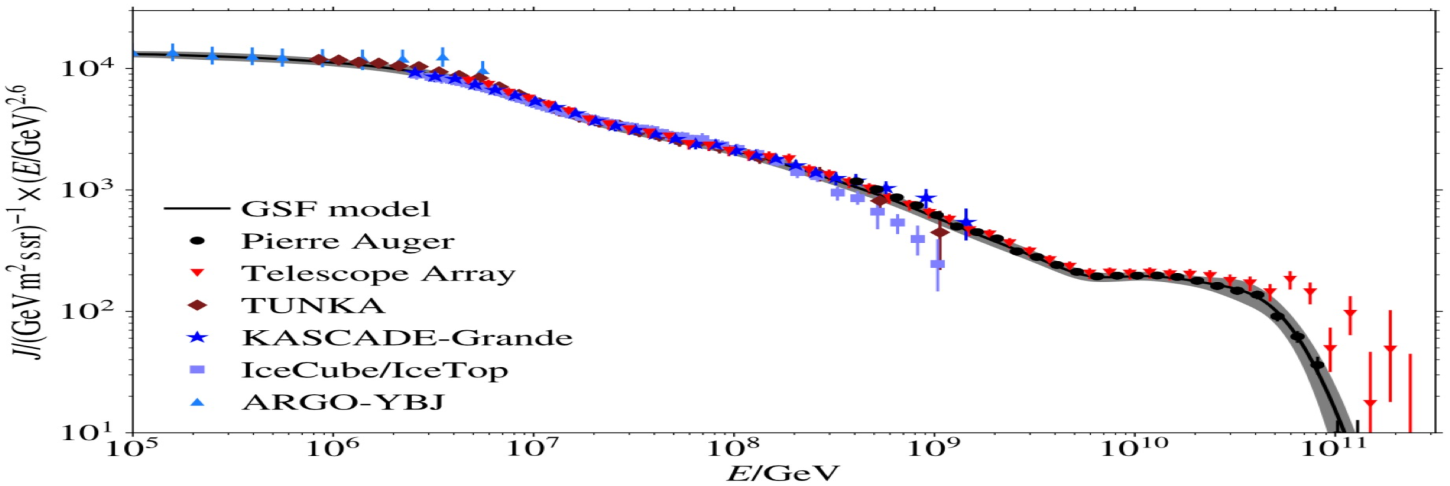

Thanks !

Systematic uncertainties: atmospheric pressure

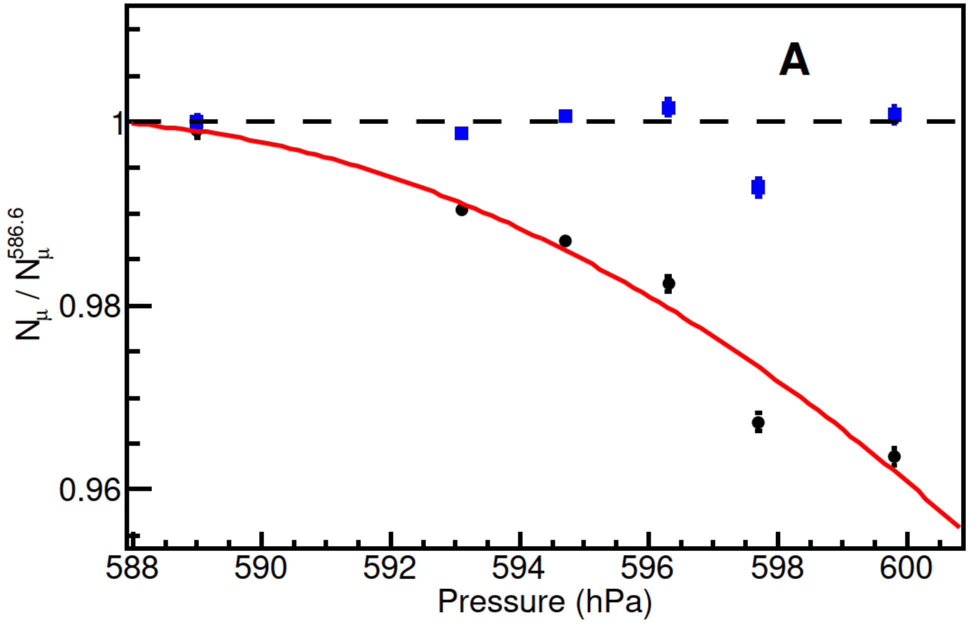

Black dot:
Data before correction
Blue square:
Data after correction
Red line:
Quadratic fitting

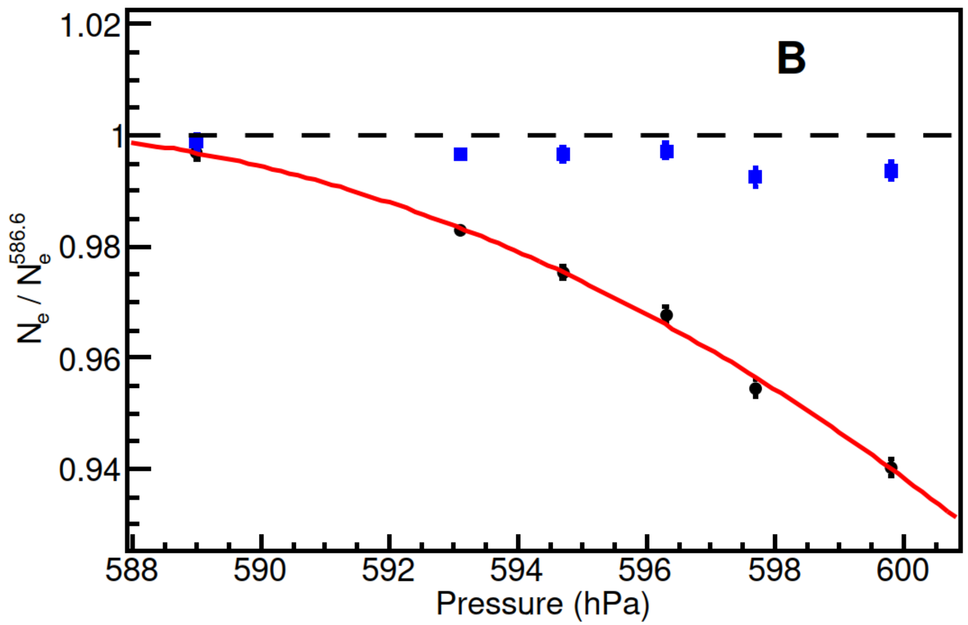

- **Correction of the effect of atmospheric pressure changes on the data**
  - **We correct Nμ and Ne to an atmospheric pressure of 586.6 hPa, which aligns with the simulation settings.**
  - **The systematic uncertainty is less than 1% after the correction.**
  - **This conclusion is based on a comparison between two data samples: one with atmospheric pressure greater than 595 hPa and the other with pressure less than 595 hPa.**

Systematic uncertainties: photons attenuation in the atmosphere

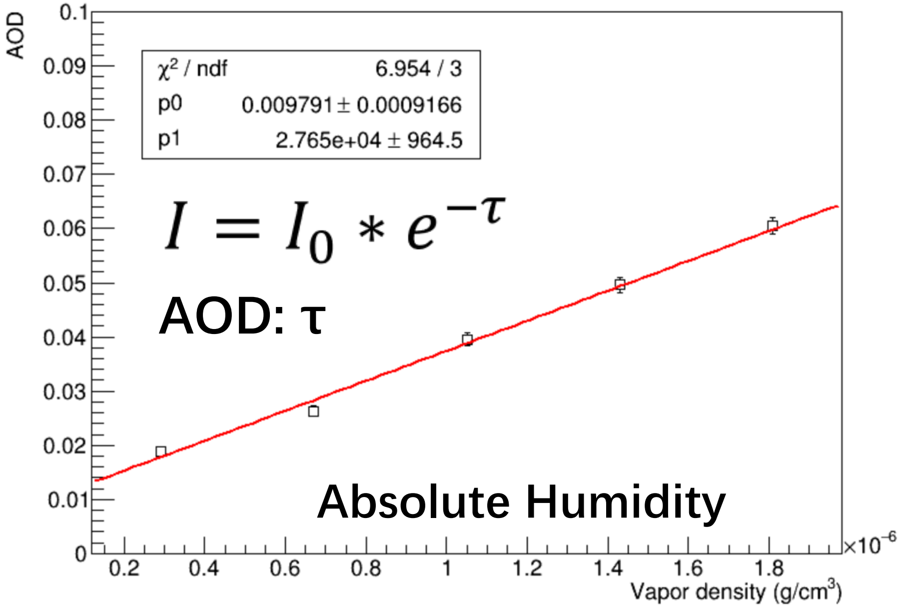

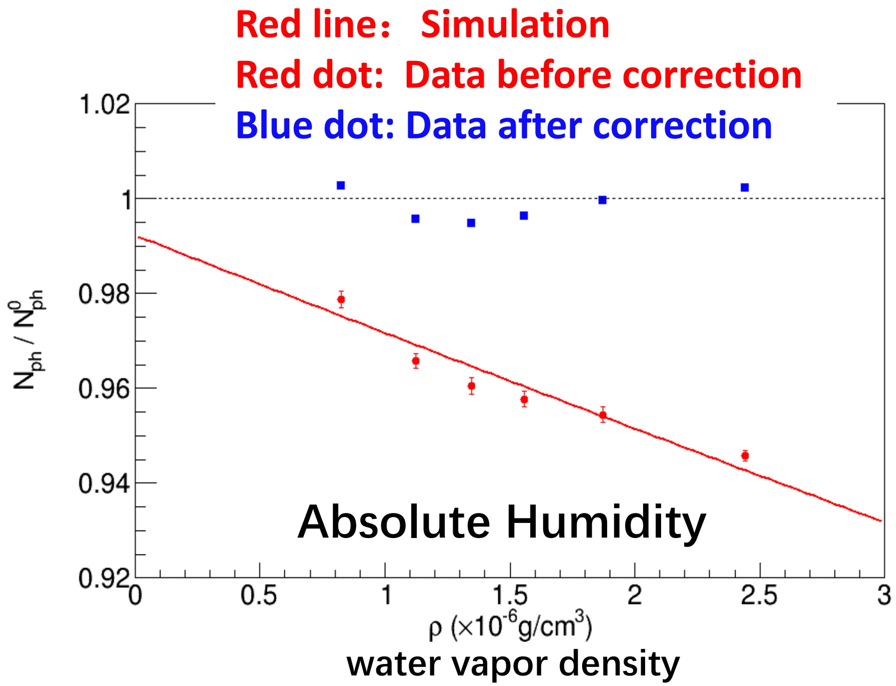

- Solar SpectralRadiometer or LHAASO site
  - To measure Aerosol Optical Depth（AOD) during the day.
  - To quantify the light absorbed and scattered by aerosols in a vertical column of the atmosphere.

- **Correction of the effect of photons attenuation in the atmosphere**
  - The main component responsible for the absorption of Cherenkov light in the atmosphere is the water vapor.
  - After water vapor correction, other components in the aerosol still maintain an absorption of about 1%, which has also been corrected in this data analysis.
  - **The systematic uncertainty is less than 1% after the correction.**

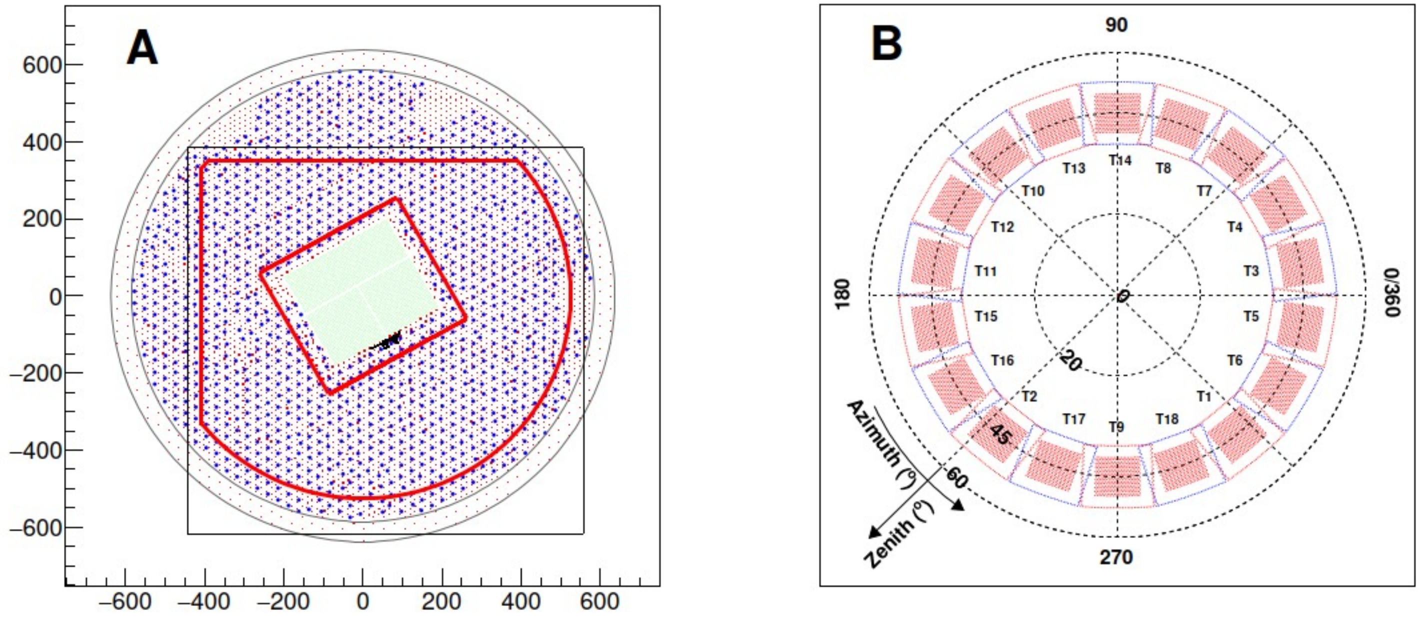

Figure S1: **LHAASO layout.** (**A**): The WCDA is located at the center of the LHAASO detector array, surrounded by the KM2A array and 18 Cherenkov telescopes of WFCTA. The red solid line marks the area for selecting the reconstructed shower core, while the black solid line denotes the throwing area for the shower core in the simulation. The distance from the core selection area to the KM2A boundary exceeds 50 meters, and the throwing area boundary is more than 30 meters away, ensuring accurate geometric reconstruction. (**B**): The dashed line represents the FoV of WFCTA. The red area represents the FoV for selecting the centroid of the Cherenkov image in the analysis.